2-Loop Functional Renormalization Group Theory of the Depinning Transition

Pierre Le Doussal[1], **Kay Jörg Wiese**[2] **and Pascal Chauve**[3]

[1] *CNRS-Laboratoire de Physique Théorique de l'Ecole Normale Supérieure, 24 rue Lhomond, 75005 Paris, France*
[2] *Institute of Theoretical Physics, University of California at Santa Barbara, Santa Barbara, CA 93106-4030, USA*
[3] *CNRS-Laboratoire de Physique des Solides, Université de Paris-Sud, Bât. 510, 91405 Orsay, France*

(Dated: May 6, 2002)

We construct the field theory which describes the universal properties of the quasi-static isotropic depinning transition for interfaces and elastic periodic systems at zero temperature, taking properly into account the non-analytic form of the dynamical action. This cures the inability of the 1-loop flow-equations to distinguish between statics and quasi-static depinning, and thus to account for the irreversibility of the latter. We prove two-loop renormalizability, obtain the 2-loop β-function and show the generation of "irreversible" anomalous terms, originating from the non-analytic nature of the theory, which cause the statics and driven dynamics to differ at 2-loop order. We obtain the roughness exponent ζ and dynamical exponent z to order ϵ^2. This allows to test several previous conjectures made on the basis of the 1-loop result. First it demonstrates that random-field disorder does indeed attract all disorder of shorter range. It also shows that the conjecture $\zeta = \epsilon/3$ is incorrect, and allows to compute the violations, as $\zeta = \frac{\epsilon}{3}(1 + 0.14331\epsilon)$, $\epsilon = 4 - d$. This solves a longstanding discrepancy with simulations. For long-range elasticity it yields $\zeta = \frac{\epsilon}{3}(1 + 0.39735\epsilon)$, $\epsilon = 2 - d$ (vs. the standard prediction $\zeta = 1/3$ for $d = 1$), in reasonable agreement with the most recent simulations. The high value of $\zeta \approx 0.5$ found in experiments both on the contact line depinning of liquid Helium and on slow crack fronts is discussed.

arXiv:cond-mat/0205108v1 6 May 2002

I. INTRODUCTION

A. Overview

Pinning of coherent structures by quenched disorder, and one of its most striking manifestations, the depinning transition, are important, ubiquitous and not fully understood phenomena[1–3]. Even a single particle in a quenched random potential exhibits a depinning threshold at zero temperature: Unbounded motion occurs only when the additional external applied force f exceeds a critical force f_c. Depinning also occurs for systems with many interacting particles, and depending on the degree of order in the structure, it ranges from the so-called plastic depinning[4] to elastic depinning. Here we focus on elastic depinning where the particles form a lattice or more generally a well ordered structure. The depinning transition is then a rather non-trivial collective phenomenon, intrinsically out of equilibrium and irreversible: It is well known for instance to be a source of hysteresis in magnets and superconductors[5].

For many experimental systems which exhibit a depinning transition a modelization in terms of an elastic object pinned by random impurities is a good starting point. The type of disorder, which they experience, depends on their symmetries and their local environment. Domain walls in magnets[6], whose study is of importance to information storage technology, behave as elastic interfaces and can experience either random-bond disorder (RB), which is short range (SR), or random-field disorder (RF), which has long range (LR) spatial correlations. Dislocation lines in metals exhibit a depinning threshold as the stress in increased[7]. Charge density waves (CDW) in solids exhibit a similiar conduction threshold. If the applied electric field becomes large enough, the CDW starts to slide[8]. Being periodic objects the disorder they feel is also periodic[9]. This is also the case for superconductors, where vortex lines form, in presence of weak disorder, a quasi ordered periodic Bragg glass phase[10,11]. These systems have similarities with (vortex free) continuous XY spins in presence of random fields, and generally constitute the random-periodic (RP) universality class.

The contact line of a liquid helium meniscus on a rough substrate can be thought of as an interface, but is governed by long range elasticity and so are slowly propagating cracks[2,12–15]. Solid friction is another example of a depinning phenomenon. Of course, in each of these systems it must be checked separately whether the elastic description holds for depinning. It is far from obvious that this is true for all relevant scales. In any case, in order to be capable to confirm or rule out such a description, it is necessary to first obtain precise theoretical predictions for the expected behavior in the case of elastic depinning, what we aim to achieve here.

It was proposed some time ago, starting from the study of a fully connected mean-field-type model[16], that the elastic depinning transition can be viewed in the framework of standard critical phenomena. The ordered phase is then the moving phase with force $f > f_c$, and the order parameter the velocity v, which vanishes as $v \sim (f - f_c)^\beta$ at the critical point $f = f_c$. The analogy with standard critical phenomena in a pure system however has some limits: Additional fluctuation exponents were later identified[9,17], and some non-universality was noticed in the fully connected model[16,18].

It is thus important to develop a renormalization-group description of depinning. An important step in that direction was performed within the framework of the so-called Functional Renormalization Group (FRG), to 1-loop order using the Wilson scheme[17,19–21]. The upper critical dimension was identified as $d_{\rm uc} = 4$, d being the internal dimension of the elastic manifold. The peculiarity of the problem is that for $d < d_{\rm uc} = 4$ an infinite set of operators becomes relevant, parameterized by a full function $\Delta(u)$, the second cumulant of the random pinning force. This problem turns out to be closely

related to the statics, i.e. describing the pinned state with minimal energy in the absence of an applied force $f = 0$ for which the FRG was initially developed[22] (there, the flowing function is the second cumulant $R(u)$ of the random potential). Both problems are notably difficult due to so-called dimensional reduction (DR) which renders the naive $T = 0$ perturbation theory useless[6,23–27]. Indeed to *any* order in the disorder at zero temperature $T = 0$, *any* physical observable is found to be *identical* to its (trivial) average in a Gaussian random force (Larkin) model. This phenomenon is not restricted to elastic manifolds in disorder, but occurs in a broad class of disordered systems as e.g. random field spin models and solving it here may open the way to a solution in other models as well. The FRG at depinning and in the statics seems to provide a way out of the DR puzzle: the key feature is that the coarse grained disorder correlator becomes *non-analytic* beyond the Larkin scale L_c, yielding large-scale results distinct from naive perturbation theory, which assumes an analytic disorder correlator. Explicit solution of the 1-loop Functional RG equation (FRG) for the disorder correlators $R(u)$ and $\Delta(u)$ gives several non-trivial attractive fixed points (FP)[10,22] and critical exponents for statics and depinning[10,17,19,21,22] to lowest order in $\epsilon = 4 - d$. All these fixed points exhibit a "cusp" singularity, which has the form $\Delta^*(u) - \Delta^*(0) \sim |u|$ at small $|u|$. The existence of the cusp nicely accounts for the existence of a critical threshold force[19], as it is found that $f_c \sim \frac{\mathrm{d}}{\mathrm{d}u}\big|_{u=0^+} \Delta^*(u)$.

There are however several highly unsatisfactory and puzzling features within the 1-loop treatment, which prompted the present and related works. First it was found that the FRG flow equation for the statics and depinning are *identical* to one loop (with $\Delta(u) = -R''(u)$). This implies for instance that, within a given universality class (RB,RF and RP), the 1-loop RG is a priori unable to distinguish static observables, such as the roughness exponent ζ at zero applied force $f = 0$ from those at depinning $f = f_c$. This is a rather surprising and unphysical result since one knows that depinning is an irreversible out of equilibrium process, quite different from the statics. In an attempt to recover the expected physics, and to extend conclusions from the 1-loop study to higher orders, three *conjectures* were put forward[17,19–21]:

1. At more than 1-loop order depinning should differ from statics.

2. At depinning the RB universality class should flow to the RF universality class: Indeed, since for $f \to f_c^+$ the manifold does not move backward it cannot feel the "potential" character of RB disorder.

3. The roughness exponent of the RF universality class at depinning is $\zeta = \epsilon/3$ to all orders (the Narayan Fisher (NF) conjecture[17,21]), with $\epsilon = 4 - d$ for standard manifold elasticity and $\epsilon = 2 - d$ for LR elasticity.

While conjectures 1 and 2 seem reasonable on physical grounds, we emphasize that they were based on qualitative arguments: In the absence of any (renormalizable) theory beyond one loop, they appear putative. A 1-loop study including the effect of a finite velocity[28] indeed indicated that 2 is correct. It strongly relies on a finite velocity, and the behavior in the limit $v = 0^+$ was found to be subtle and difficult to fully control within that approach.

The NF conjecture 3 is based on a study of the structure of higher orders, but it lacks a controlled field theory argument. With the time, it got more and more in disagreement with numerical simulations and experiments, as we discuss below. In addition, if one considers that this value $\zeta = \epsilon/3$ is expected instead for the *statics* RF class, the NF conjecture seems rather unnatural.

There are also more fundamental reasons to study the FRG beyond one loop. In the last fifteen years since[16,22], no study has addressed whether the FRG yields, beyond one loop, a renormalizable field theory able to predict universal results. There have been 2-loop studies previously but they assumed an analytic correlator and thus they only applied below the Larkin length[29–31]. Doubts were even raised[32] about the validity of the ϵ-expansion beyond order ϵ.

The aim of the present paper is to develop a more systematic field theoretic description of depinning which extends beyond one loop. A short summary of our study was already published[33] together with a companion study on the statics. The main and highly non-trivial difficulty is the non-analytic nature of the theory (i.e. of the fixed-point action) at $T = 0$, which makes it a priori quite different from conventional critical phenomena. It is not even obvious whether this is a legitimate field theory and how to construct it. For the depinning transition with $f = f_c^+$, which is the focus of the present paper, we are able to develop a meaningful perturbation theory in a non-analytic disorder which allows us to show renormalizability at 2-loop order. Even the way renormalizability works here is slightly different from the conventional one. To handle the non-analyticity in the static problem is even more challenging, and we propose a solution of the problem to 2-loop[33,34] and 3-loop[35] order as well as at large-N [36].

In this paper we focus on the so-called "isotropic depinning" universality class. This means that the starting model has sufficient rotational invariance, as discussed below, which guarantees that additional Kardar-Parisi-Zhang terms are absent. A general discussion of the various universality classes can be found in[37,38] and an application of our non-analytic field theory (NAFT) methods to the case of "anisotropic depinning" will be presented in[39].

Before we summarize the novel results of the present paper, let us recall some important features about the model, the scaling and statistical fluctuations at the depinning threshold.

B. Model, scaling and fluctuations

Elastic objects can be parameterized by a N-component height or displacement field u_x, where x denotes the d-dimensional internal coordinate of the elastic object (we will use u_q to denote Fourier components). An interface in the 3D random field Ising model has $d = 2$, $N = 1$, a vortex lattice $d = 3$, $N = 2$, a contact-line $d = 1$ and $N = 1$. In this paper we restrict our study to $N = 1$. In the presence of a random potential the equilibrium problem is defined by the

Hamiltonian:

$$\mathcal{H} = \int_q \frac{c(q)}{2} u_q u_{-q} + \int_x V(u_x, x) \tag{I.1}$$

with $c(q) = cq^2$ for standard short-range elasticity, $c(q) = c|q|$ for long-range elasticity and we denote $\int_q = \int \frac{d^d q}{(2\pi)^d}$ and $\int_x = \int \mathrm{d}^d x$. Long-range elasticity appears e.g. for the contact line by integrating out the bulk-degrees of freedom[40]. For periodic systems the integration is over the first Brillouin zone. More generally a short scale UV cutoff is implied at $q \sim \Lambda$, and the system size is denoted by L. As will become clear later, the random potential can without loss of generality be chosen Gaussian with second cumulant

$$\overline{V(u,x)V(u',x')} = R(u-u')\delta^d(x-x') \; . \tag{I.2}$$

Periodic systems are described by a periodic function $R(u)$, random bond disorder by a short range function and random field disorder of amplitude σ by $R(u) \sim -\sigma|u|$ at large u.

We study the over-damped dynamics of the manifold in this random potential, described (in the case of SR-elasticity) by the equation of motion

$$\eta \partial_t u_{xt} = c\nabla_x^2 u_{xt} + F(x, u_{xt}) + f \tag{I.3}$$

with friction η. In presence of an applied force f the center of mass velocity is $v = L^{-d}\int_x \partial_t u_{xt}$. The pinning force is $F(u,x) = -\partial_u V(u,x)$ and thus the second cumulant of the force is

$$\overline{F(x,u)F(x',u')} = \Delta(u-u')\delta^d(x-x') \; , \tag{I.4}$$

such that $\Delta(u) = -R''(u)$ in the bare model. As we will see below it does not remain so in the driven dynamics. The "isotropic depinning" class contains more general equations of motion than (I.3). For instance some cellular automaton models are believed to be in this class[41]. They must obey rotational invariance, as discussed in Ref.[37–39], which prevents the additional KPZ term $\lambda(\nabla_x u_{xt})^2$ to be generated at $f = f_c^+$. There is always a KPZ term generated at $v > 0$ from the broken symmetry $x \to -x$, but λ can vanish or not as $v \to 0^+$, depending on whether rotational invariance is broken or not. Here this symmetry is implied by the statistical tilt symmetry (STS)[42,43] $u_{xt} \to u_{xt} + g_x$. It also holds in the statics and accounts for the non-renormalization of the elastic coefficient, here set to $c = 1$.

A quantity measured in numerical simulations and experiments is the roughness exponent at the depinning threshold $f = f_c$

$$C_L(x-x') = \overline{|u(x) - u(x')|^2} \sim |x-x'|^{2\zeta} \; , \tag{I.5}$$

which can be compared to the static one ζ_{eq}. Other exponents have been introduced[16,17,19–21]. The velocity near the depinning threshold behaves as $v \sim (f-f_c)^\beta$; the dynamical response scales with the dynamical exponent $t \sim x^z$ and the local velocity correlation length ξ diverges at threshold with $\xi \sim (f-f_c)^{-\nu}$. There have also been some studies below threshold[9,44]. The following exponent relations were found to hold[19]:

$$\beta = \nu(z-\zeta) \tag{I.6}$$

$$\nu = \frac{1}{2-\zeta} \tag{I.7}$$

the latter using STS. There are various ways to measure the roughness exponent. In some simulations[45–47] it has been extracted from the critical configuration, i.e. as f is increased to f_c in a given sample it is obtained from the last blocking configuration. It can also be defined as the limit $v \to 0^+$ of the roughness in the moving state, which we will refer to as the "quasi-static" depinning limit to distinguish it from the previous one. This is the situation studied in this paper. Although it is widely believed that both are the same, the depinning theory has enough peculiarities that one should be careful. In particular, beyond scaling arguments and simulations, there is presently no rigorous method capable to connect the behavior below and above threshold.

Another peculiarity was noted in[17]. It was found that the finite-size fluctuations of the critical force can scale with a different exponent:

$$f_c(L) - f_c \sim L^{-1/\nu_{\mathrm{FS}}} \tag{I.8}$$

and it was questioned whether $\nu_{\mathrm{FS}} = \nu$. The bound

$$\nu_{\mathrm{FS}} \geq 2/(d+\zeta) \tag{I.9}$$

follows from a general argument of Ref.[48]. For charge density waves where $\zeta = 0$ one sees that $\nu = 1/2$ and thus ν and ν_{FS} must be different for $d < 4$. For interfaces it was noted[17] that $\nu = \nu_{\mathrm{FS}}$ is possible provided $\zeta \geq \epsilon/3$. If one assumes $\nu = \nu_{\mathrm{FS}}$, the NF-conjecture $\zeta = \epsilon/3$ is then equivalent to saturating the bound (I.9). We will address the question of whether $\nu = \nu_{\mathrm{FS}}$ below.

Finally note that at $f = f_c$ the condition of equilibrium of a piece of interface expresses that the elastic force, which acts only on the perimeter, balances the excess force on the bulk, yielding the scaling:

$$L^{d-1} u(a,L) \sim (f_c(L) - f_c) L^d \; , \tag{I.10}$$

where $u(a,L) \sim \sqrt{C_L(a)}$ is the relative displacement (I.5) between two neighbors averaged over the perimeter. This shows that

$$u(a,L) \sim L^{1-\frac{1}{\nu_{\mathrm{FS}}}} \tag{I.11}$$

thus for CDW the displacements between two neighbors grows unboundedly[49] with L for $d \leq 2$. For interfaces (non-periodic disorder), if one assumes $\nu = \nu_{\mathrm{FS}}$ one obtains that the displacements between two neighbors grows with L only when $\zeta > 1$.

C. Summary of results

Let us now discuss the main results of our study.

First we show that, at depinning, 1- and 2-loop diagrams can be computed using a non-analytic action in an unambiguous and well defined way, allowing to escape dimensional reduction. The mechanism is non-trivial and works because the manifold only moves forward in the steady state which allows to remove all ambiguities. We show that the limit $v \to 0^+$ can be taken safely without additional unexpected singularities arising in this limit.

Next we identify the divergences in the 2-loop diagrams using dimensional regularization in $d = 4 - \epsilon$. We identify the 1-loop and 2-loop counter-terms and perform the renormalization program. We find that the $1/\epsilon$ divergences cancel nicely in the β-function for the disorder correlator and in the dynamical exponent. The theory is finite to 2-loop order and yields universal results.

The obtained FRG flow equation for the disorder (the β-function) contains new "anomalous" terms, absent in an analytic theory (e.g. in the flow obtained in Ref.[29,30]). These terms are different in the static theory (obtained in[33]) and at depinning, showing that indeed *static and depinning differ to two loops.* **Thus the minimal consistent theory for depinning requires two loops.**

Next we study the fixed point solutions of our 2-loop FRG equations at depinning. For non-periodic disorder (e.g. interfaces) with correlator of range shorter or equal to random-field, we find that there is a single universality class, the random-field class. Thus random-bond disorder does flow to random field. Specifically we find that the flow of $\int \Delta$ is corrected to two loops and thus $\int \Delta$ cannot remain at its random-bond value, which is zero. This is explained in more detail in section IV. The problem does not remain potential and irreversibility is manifest. For short range elasticity, we find the roughness-exponent at depinning:

$$\zeta = \frac{\epsilon}{3}\Big(1 + 0.143313\,\epsilon\Big) \tag{I.12}$$

with $\epsilon = 4 - d$, and for long range elasticity:

$$\zeta = \frac{\epsilon}{3}\Big(1 + 0.39735\,\epsilon\Big) \tag{I.13}$$

with $\epsilon = 2 - d$. Thus the NF-conjecture[17,21] that $\zeta = \frac{\epsilon}{3}$ is incorrect. We also compute the dynamical exponent z and obtain β and ν by the scaling relations (I.6) and (I.7). We also find that $\nu_{\rm FS} = \nu$ holds to two loops.

For periodic disorder, relevant for charge density waves, we find a fixed point which leads to a universal logarithmic growth of displacements. This fixed point is however unstable, as an additional Larkin random force is generated. The true correlations are the sum of this logarithmic growth and of a power law growth so that the true $\zeta = (4 - d)/2$. This is similar to[50]. Then we find

$$\nu = \frac{1}{2} \tag{I.14}$$

$$\nu_{\rm FS} = \frac{2}{d}\,, \tag{I.15}$$

which holds presumably to all orders.

D. Numerical simulations and experiments

Over many years, numerous simulations near depinning[19,20,51–54] accumulated evidence that $\zeta \neq \epsilon/3$. In $d = 1$ in particular often an exponent $\zeta > 1$ was observed. Our results show that $\zeta > \epsilon/3$ and thus resolve this long standing discrepancy between numerical simulations and the renormalization group. They are summarized in Tables IV.2 and IV.3 in Section IV, where we compare them to numerical simulations. Of course it is not possible to give strict error bars from the FRG calculation without further knowledge of higher orders, but one can still give rough estimates, based on different Padé-approximants.

Let us in the following discuss recent numerical results. Following shortly our paper[33], Rosso and Krauth obtained a set of precision numerical results using a powerful algorithm to determine the critical configuration at depinning (the last blocking configuration) up to large sizes[45–47]. They obtained results in $d = 1$ which, despite being far from $d = 4$, compare well with our results. For short range elasticity they find

$$\zeta = 1.17 \tag{I.16}$$

close to our 2-loop result (I.12). Note that displacement correlations scaling as

$$\overline{u_q u_{-q}} \sim q^{-(d+2\zeta)} \tag{I.17}$$

with $\zeta > 1$ are perfectly legitimate. It simply means that

$$C_L(x) \sim 2\int_q (1 - \cos(qx)) q^{-(d+2\zeta)} \sim L^{2(\zeta-1)} x^2\,. \tag{I.18}$$

The size dependent factor comes from the infrared divergence of the integral. Thus in a simulation neighboring monomers will be spread further and further apart, which is fine if their attraction is purely quadratic. Of course in a realistic physical situation their bond will eventually break, but as a model it is mathematically well defined. For the anisotropic depinning universality class, not studied here, they found $\zeta = 0.63$ as many other authors using cellular automaton models[55–57].

For isotropic depinning with long range elasticity they obtained:

$$\zeta = 0.390 \pm 0.002\,, \tag{I.19}$$

which lies roughly at midpoint of the 1-loop and 2-loop prediction setting $\epsilon = 1$ in (I.13). So do their most recent estimates[58] for SR disorder. In $d = 2$ this is $\zeta = 0.753 \pm 0.002$ and for $d = 3$ they obtain $0.35 < \zeta < 0.4$. These results (I.16) and (I.19) are close to estimates from the 2-loop expansion and clearly rule out the NF-conjecture.

Another recent work[59] studies an interface in the random field Ising model in high dimension. The authors confirm that $d = 4$ is the upper critical dimension. They further extract the velocity exponent β and compare their results with our 2-loop FRG prediction for β:

$$\beta = 1 - \frac{\epsilon}{9} + 0.040123\epsilon^2\,. \tag{I.20}$$

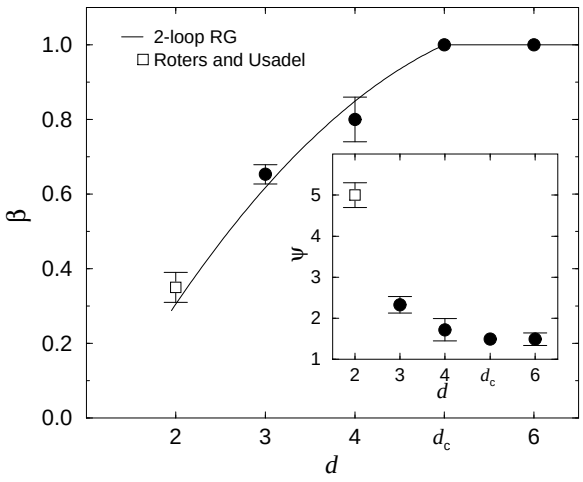


FIG. I.1: Figure from Ref.[59] which compares new numerical values (black circles) and a previous one (white square) obtained for the exponent β with our prediction from the FRG.

The results are shown in Fig. I.1. One can see a clear curvature downwards and that the straight line giving the 1-loop result is well above the obtained results (the 1-loop approximation would predict $\beta = 0.78$ in $d = 2$).

Thus, although there is still some spread and uncertainty in the results, it seems that there is now a trend towards a convergence between theory and numerical simulations.

The situation concerning experiments is presently unclear. Let us first outline the generic findings before analyzing the details. The measured exponents corresponding to LR-elasticity and $d = 1$ seem to be consistently in the range $\zeta \approx 0.5 - 0.55$. This is slightly above our 2-loop result (I.13) but not fully incompatible with it. Our calculation holds for quasi-static depinning, i.e. $v > 0 \to 0^+$, and most experiments are also performed from the moving side, hopefully reaching the same quasi-static limit $v \to 0^+$. On the other hand if one believes that the numerical result I.19 (also compatible with our calculation, from below) obtained for $f = f_c^-$ also holds for quasi-static depinning (a rather natural, but as yet unproved assumption) then one must conclude that the elastic models, in their simplest form at least, may not faithfully represent the experimental situation. Care must however be exercised before any such conclusion is reached. One could argue that disorder $\Delta(u) \sim u^{-\alpha}$ of range longer than RF ($\alpha < 1$) could produce higher exponents $\zeta = \epsilon/(2 + \alpha)$ (see end of Section IV A) but that does not seem to apply to those experiments where disorder is well controlled. Also, since the exponent $\zeta = 0.5$ is the Larkin DR-exponent, which should hold below the Larkin length L_c one must make sure that L_c is well identified and that one is not simply observing a slow crossover to the asymptotic regime. In some of these experiments L_c has been identified to be rather small.

Let us now examine the situation in more details.

One much studied experimental system is the contact line of a fluid[12,60]. It advances on a rough substrate and is pushed by adding fluid to the reservoir. The elasticity of the line is short range at short scale but at larger scales it is mediated by the elasticity of the two dimensional meniscus and thus it becomes long range and should be compared with (I.13), (I.19). Disorder is random-field, but one should distinguish between microscopic disorder, which is poorly characterized, and macroscopic one which is well controlled. The situation has been studied for a helium meniscus on a macroscopically disordered substrate where $\zeta = 0.55$ was found[60]. Although there are good indications that these experiments probe quasi-static depinning (the contact line jumps from a reproducible pinned configuration to the next one) the precise nature of the dynamics remains open. Indeed it was found that propagation of perturbations along the line can be as fast as avalanches, showing inertial regime for helium[68]. Experiments were repeated for viscous liquids[69] yielding $\zeta = 0.51 \pm 0.03$. There it was checked that the system is over-damped and near depinning. In both cases there is also evidence of thermal activation effects[13] characteristic of depinning (not creep). It was argued that these may be a signature that a more complicated dynamics (e.g. plastic) takes place at the very short scales and produces an effective dynamics at larger scales with complicated non-linear (e.g. exponential) velocity and temperature dependent damping. Very similar effects have also been shown to occur in solid friction[70] were the activation volume was also found to correspond to microscopic scales.

Another class of much studied experimental systems are crack fronts in heterogeneous media[71]. These are characterized by two displacement fields, one out-of-plane component h and an in-plane one f. Cracks can either be studied stopped or slowly advancing. At the simplest level the in-plane displacement f is expected to be described as an elastic line $d = 1$, $N = 1$ with LR elasticity $c|q|$, at quasi static depinning[72]. In experiments[15,73] the observed roughness is again $\zeta_f \approx 0.55$. Since the crack propagates in an elastic medium, elastic waves which can in principle affect the roughness as the crack front advances producing a more complicated dynamics than Eq. (I.3). Some proposals have been put forward on mechanisms to produce higher roughness exponents[74] They rely however on a finite velocity and it is unclear whether they can modify roughness in the quasi-static limit. Even if instantaneous velocities during avalanches become large enough, a detailed description on how these could change the line configurations remains to be understood. Then of course a major issue is whether the experiment, and in which sense, is in the quasi-static limit. There again microscopic dynamics could be more complex as at small scales the material may be damaged and the notion of a single front may not apply. Finally, since there are two components to displacement one should also be careful to understand interactions between them near depinning[61].

Another interesting experimental system is a domain wall in a very thin magnetic film[62] which experiences RB disorder. Up to now however only the thermally activated motion has been studied, which gives a quite remarkable confirmation of the creep law[62] with RB exponents. It would be interesting to study depinning there and to check whether it also belongs to the isotropic universality class. In that case, the crossover

from RB to RF resulting in overhangs beyond some scale at zero temperature ($\zeta > 1$) as well as the non-trivial thermal rounding of depinning could be studied.

II. MODEL AND PERTURBATION THEORY

In this Section we discuss some general features of the field theory of elastic manifolds in a random potential, both for the statics and for the dynamics, driven or at zero applied force. Some issues are indeed common to these three cases. At the end we specialize to depinning.

A. Static and Dynamical action and naive power counting

The static, equilibrium problem, can be studied using replicas. The replicated Hamiltonian corresponding to (I.1) is:

$$\frac{\mathcal{H}}{T} = \frac{1}{2T}\int_x \sum_a [(\nabla u_x^a)^2 + m^2 u_x^a] - \frac{1}{2T^2}\int_x \sum_{ab} R(u_x^a - u_x^b)\,, \tag{II.1}$$

where, for now, we consider SR elasticity. a runs from 1 to n. We have added a small mass to provide an infrared cutoff, and we are interested in the large scale limit $m \to 0$. The limit of zero number of replicas $n = 0$ is implicit everywhere. Terms with sums over three replicas or more corresponding to third or higher cumulants of disorder are generated in the perturbation expansion. These should in principle be included, but as we will see below higher disorder cumulants are not relevant for the $T = 0$ depinning studied below.

The dynamics, corresponding to the equation of motion (I.3) is studied using the dynamical action averaged over disorder:

$$\mathcal{S}[\hat{u}, u] = \int_{xt} i\hat{u}_{xt}(\eta\partial_t - \partial_x^2 + m^2)u_{xt} - \eta T\int_{xt} i\hat{u}_{xt} i\hat{u}_{xt} - \frac{1}{2}\int_{xtt'} i\hat{u}_{xt} i\hat{u}_{xt'}\Delta(u_{xt} - u_{xt'}) - \int_{xt} i\hat{u}_{xt} f_{xt}\,. \tag{II.2}$$

It generates disorder averaged correlations, e.g. $\overline{\langle A[u_{xt}]\rangle} = \langle A[u_{xt}]\rangle_S$ with $\langle A\rangle_S = \int \mathcal{D}[u]\mathcal{D}[\hat{u}] A \mathrm{e}^{-S}$ and $\langle 1\rangle_S = 1$, and response functions $\overline{\delta\langle A[u]\rangle/\delta f_{xt}} = \langle i\hat{u}_{xt} A[u]\rangle_S$. The uniform driving force $f_{xt} = f > 0$ (beyond threshold at $T = 0$) may produce a velocity $v = \overline{\partial_t\langle u_{xt}\rangle} > 0$, a situation which we study by going to the comoving frame (where $\overline{\langle u_{xt}\rangle} = 0$) shifting $u_{xt} \to u_{xt} + vt$, resulting in $f \to f - \eta v$. This is implied below. In general, for any value of f, we study the steady state, which at finite temperature $T > 0$ is expected to be unique and time translational invariant (TTI) (all averages depend only on time differences). In the zero temperature limit, one needs a priori to distinguish the $T = 0$ TTI theory as $\lim_{L\to\infty}\lim_{T\to 0}$ (e.g. the ground state in the static) and the $T = 0^+$ theory as $\lim_{T\to 0}\lim_{L\to\infty}$.

It is important to note that there are close connections, via the fluctuation dissipation relations, between the dynamical formalism and the statics. Indeed, at equilibrium (for $f = 0$ and when time translation invariance is established) any equal time correlation function computed with (II.2) is formally identical (e.g. to all orders in perturbation theory) to the corresponding quantity computed in the equilibrium theory (which is a single replica average). Similarly, the persistent parts, i.e. those $\propto \delta(\omega)$, of dynamical correlations involving p mutually very separated times, are formally identical to the corresponding averages in the replica theory involving p replicas. The perturbative equilibrium calculations in the statics can thus be indifferently performed either with replicas or with (II.2). It is possible to generate all dynamical graphs from static ones, a connection which, as will be further explained below, also carries to some extent to the case $f > 0$ at $T = 0$.

We first study "naive" perturbation theory and power counting. The quadratic part S_0 of the action (II.2) yields the free response and correlation functions, used for perturbation theory in the disorder. They read

$$\langle i\hat{u}_{q,t'} u_{-q,t}\rangle_0 = R_{q,t-t'} = \frac{\theta(t-t')}{\eta}\mathrm{e}^{-\frac{(t-t')}{\eta}(q^2+m^2)}$$
$$\langle u_{q,t'} u_{-q,t}\rangle_0 = C_{q,t-t'} \tag{II.3}$$

respectively, with the FDT relation $TR_{q,\tau} = -\partial_\tau C_{q,\tau}$ ($\tau > 0$). Perturbation theory in $\Delta(u)$ yields a disorder interaction vertex and at each (unsplitted) vertex there is one conservation rule for momentum and two for frequency. It is thus convenient to use splitted vertices, as represented in Fig II.1, where the rules for the perturbation theory of the statics using replica are also given. For the dynamics one can also focus on $T = 0$ where graphs are made only with response functions and consider temperature as an interaction vertex. The 1-loop and 2-loop diagrams which correct the disorder at $T = 0$ are shown in Fig. II.1 (unsplitted vertices). There are three types of 2-loop graphs A, B, C. The graphs E and F lead to corrections proportional to temperature.

At $T = 0$ the model exhibits the property of dimensional reduction[6,23–27] (DR) both in the statics and dynamics. Its "naive" perturbation theory, obtained by taking for the disorder correlator $\Delta(u)$ an *analytic function* of u (or $R(u)$ for the statics), has a triviality property. As is easy to show using the above diagrammatic rules the perturbative expansion of any correlation function $\langle\prod_i u_{x_i t_i}\rangle_S$ in the derivatives $\Delta^{(n)}(0)$ yields to all orders the same result as that obtained from the Gaussian theory setting $\Delta(u) \equiv \Delta(0)$ (the so called Larkin random force model). The same result holds for the statics, for any correlation $\langle\prod_i u_{x_i}^{a_i}\rangle_S$. At $T = 0$ these correlations are independent of the replica indices a_i, their dynamical equivalent being independent of the times t_i. The two point function thus reads to all orders:

$$\overline{\langle u_{q,t'} u_{-q,t}\rangle}_{\mathrm{DR}} = \frac{\Delta(0)}{(q^2+m^2)^2}\,. \tag{II.4}$$

This dimensional reduction results in a roughness exponent $\zeta = (4-d)/2$ which is well known to be incorrect. One physical reason, in the statics, is that this amounts to solving the zero force equation which, whenever more than one solution exists, is not identical to finding the lowest energy

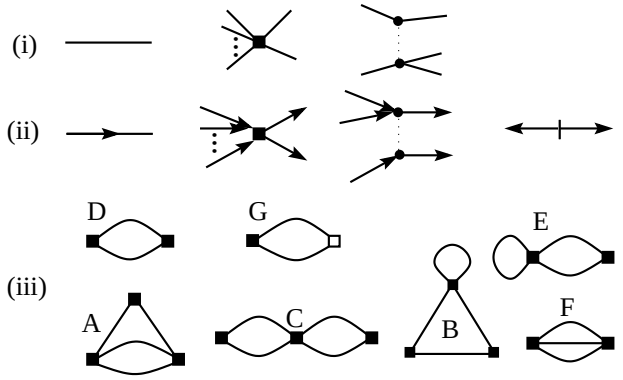


FIG. II.1: (i) diagrammatic rules for the statics: replica propagator $\langle u_a u_b\rangle_0 \equiv T\delta_{ab}/q^2$, unsplitted vertex, equivalent splitted vertex $-\sum_{ab}\frac{1}{2T^2}R(u_a-u_b)$ and (ii) dynamics: response propagator $\langle \hat{u}u\rangle_0 \equiv R_{q,t-t'}$, unsplitted vertex, splitted vertex $\hat{u}_{xt}\hat{u}_{xt'}\Delta(u_{xt}-u_{xt'})$ and temperature vertex. Arrows are along increasing time. An arbitrary number of lines can enter these functional vertices. (iii) unsplitted diagrams to one loop D, one loop with inserted 1-loop counter-term G and 2-loop A,B,C,E,F.

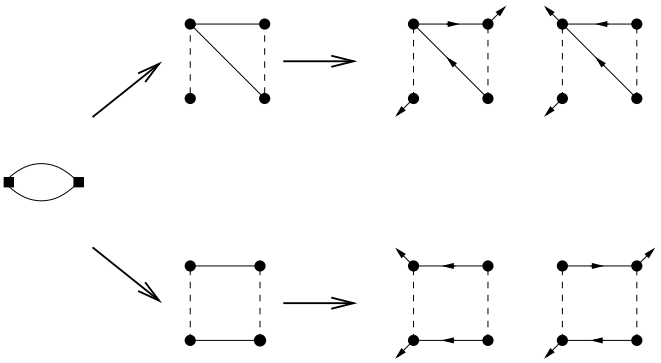


FIG. II.2: Construction of diagrams starting from an unsplitted static diagram via two splitted static diagrams (2-replica component) to the corresponding dynamical diagrams as explained in the text.

configuration. Curing this problem, within a field theory, is highly non-trivial. One way to do that, as discussed later will be to consider a *non-analytic* $\Delta(u)$.

It is important to note that despite the DR, dynamical averages involving response fields remain non-trivial, even at zero temperature. Perturbation theory at finite temperature also remains non-trivial. It is thus still useful to do power counting with an analytic $\Delta(u)$, the modifications for a non-analytic $\Delta(u)$ being discussed in the following section.

Power counting at the Gaussian fixed point yields $t \sim x^2$ and $\hat{u}u \sim x^{-d}$. At $T = 0$ nothing else fixes the dimensions of u, since $u \to \lambda u$, $\hat{u} \to \lambda^{-1}\hat{u}$ leaves the $T = 0$ action invariant. Denoting $u \sim x^{\zeta}$, ζ is for now undetermined. The disorder term then scales as $x^{4-d+2\zeta}$. It becomes relevant for $d < 4$ provided $\zeta < (4-d)/2$ which is physically expected (for instance in the random periodic case, $\zeta = 0$ is the only possible choice, and for other cases $\zeta = O(\epsilon)$). With this power counting the temperature term scales as $x^{-\theta}$ with $\theta = d-2+2\zeta$ and is thus formally irrelevant near four dimension. In the end ζ will be fixed by the disorder distribution at the fixed point[22].

A more detailed study of divergences in the vertex functions allows to identify all counter-terms needed to render the theory finite. We denote by

$$\Gamma_{\hat{u}..\hat{u};u..u}(\hat{q}_i,\hat{\omega}_i,q_i,\omega_i) = \prod_{i=1}^{E_u}\frac{\delta}{\delta u_{q_i,\omega_i}}\prod_{j=1}^{E_{\hat{u}}}\frac{\delta}{\delta \hat{u}_{\hat{q}_j,\hat{\omega}_j}}\Gamma[u,\hat{u}]\Big|_{u=\hat{u}=0} \quad \text{(II.5)}$$

the irreducible vertex functions (IVF) with E_u external fields u (at momenta q_i, ω_i, $i = 1,..E_u$) and $E_{\hat{u}}$ external fields (at momenta $\hat{q}_i, \hat{\omega}_i$, $i = 1,..E_{\hat{u}}$). Being the derivative of the effective action functional $\Gamma[u,\hat{u}]$ they are the important objects since all averages of products of u and $\hat{u}$ fields are expressed as tree diagrams of the IVF. Finiteness of the IVF thus imply finiteness of all such averages. The present theory has the property of covariance under the well known statistical tilt symmetry STS $u_{xt} \to u_{xt} + g_x$, which yields that the two point vertex $\Gamma_{\hat{u}u}(\omega = 0)$ remains uncorrected to all orders. This allows to fix the elastic constant $c = 1$ and shows that the mass term is uncorrected and can thus safely be used as an IR cutoff. It also implies that all higher IVFs vanish when any of the ω_i is set to zero. The DR result is a perturbative triviality statement about $\Gamma_{\hat{u}..\hat{u}}(\hat{q}_i,\hat{\omega}_i)$ at $T = 0$, all other cases remain non-trivial. In a sense we will now expand around dimensional reduction. Similar replica IVFs can be defined for the statics.

Perturbation expansion of a given IVF to any given order in the disorder can be represented by a set of one particle irreducible (1PI) graphs. As mentionned above there is a simple rule to generate the dynamical graphs from the static ones. The static propagator being diagonal in replicas, each static graph occurring in a p replica IVF contains p connected components. At $T = 0$ the rule is then to attach one response field to each connected component of the static diagram, each replica graph then generating one or more dynamical graphs. The place where the response field is attached is the *root* of the diagram. The direction of the remaining response functions is then fixed unambiguously, always pointing towards the root. This procedure to deduce the dynamical diagrams from the static ones is *unique* and *exhaustive* and is illustrated in Fig. II.2. A generalization exists at $T > 0$ but is not needed here.

Any graph corresponding to a given dynamical IVF contains p connected components (in the splitted diagrammatics) with $1 \le p \le E_{\hat{u}}$ ($p = E_{\hat{u}}$ at $T = 0$), each one leading to a conservation rule between external frequencies, and thus one can write symbolically:

$$\Gamma_{\hat{u}..\hat{u};u..u}(\hat{q}_i,\hat{\omega}_i,q_i,\omega_i) = \delta\Big(\sum\hat{q}-\sum q\Big)\prod_{i=1}^{p}\delta\Big(\sum\hat{\omega}-\sum\omega\Big)\tilde{\Gamma}\,. \quad \text{(II.6)}$$

Let us compute the superficial degree of UV divergence α of such a graph with v_Δ disorder vertices and v_T temperature factors contributing to $\tilde{\Gamma} \sim \Lambda^{\alpha}$. Using momentum and frequency conservation laws at each vertex, and since there are

only response functions $E_{\hat{u}} + I = 2(v_\Delta + v_T)$ we obtain:

$$\alpha = d + 2p - dE_{\hat{u}} + (d-4)v_\Delta + (d-2)v_T \ . \quad \text{(II.7)}$$

At $T = 0$ ($v_T = 0$, $p = E_{\hat{u}}$) at the critical dimension $d = 4$ the only superficially UV divergent IVF are those with one external $\hat{u}$ (quadratic divergence) or two external $\hat{u}$ (logarithmic divergence LD). The STS further restricts the possible divergent diagrams. One sees that only three types of counter-term are needed a priori. One counter-terms is needed for the Λ^2 divergence of $\Gamma_{\hat{u}}(q = 0, \omega = 0)$ (excess force $f - \eta v$ in driven dynamics). This is analogous to the mass in the ϕ^4 theory, i.e. the distance to criticality. If we are exactly at the depinning critical point ($f = f_c$) we need not worry about this divergence. Another counter-term is associated with the LD in η and the last one with the LD in the second cumulant of disorder $\Delta(u)$, i.e. a full function, which makes it different from the conventional FT for critical phenomena (e.g. ϕ^4). One notes that higher cumulants are formally irrelevant, as they involve $E_{\hat{u}} > 2$.

One sees from (II.7) that each insertion of a temperature vertex yields an additional quadratic divergence in $d = 4$, more generally a factor $T\Lambda^{d-2}$. Thus to obtain a theory where observables are finite as $\Lambda \to \infty$ one must start from a model where the initial temperature scales with the UV cutoff as

$$T = \tilde{T} m^{-\theta} \left(\frac{m}{\Lambda}\right)^{d-2} \ . \quad \text{(II.8)}$$

This is similar to the ϕ^4 theory where it is known that a ϕ^6 term can be present and yields a finite UV limit (i.e. does not spoil renormalizability) only if it has the form $g_6\phi^6/\Lambda^{d-2}$. It then produces only a finite shift to g_4 without changing universal properties[75]. Here each $\tilde{T}$ factor will thus come with a Λ^{2-d} factor which compensates the UV divergence. Computing the resulting shift in $\Delta(u)$ to order Δ^2 by resumming the diagrams E and F of Fig. II.1 and all similar diagrams to any number of loops has not been attempted here.

For convenience we have inserted factors of m in the definition of the rescaled temperature, using the freedom to rescale u by $m^{-\zeta}$ and $\hat{u}$ by m^{ζ}. The disorder term then reads as in (II.2) with $\Delta(u)$ replaced by $\Delta_0(u) = m^{\epsilon-2\zeta}\tilde{\Delta}(um^{\zeta})$ in terms of a dimensionless rescaled function $\tilde{\Delta}$.

B. Non-analytic field theory and depinning in the quasi-static limit

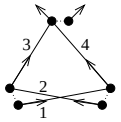
From now on we study the zero temperature limit $T = 0$. To escape the DR triviality phenomenon, and since the fixed points found in 1-loop studies exhibit a cusp at $u = 0$, we must consider perturbation theory in a *non-analytic* disorder correlator. In this section we show how to develop perturbation theory and diagrammatics in a non-analytic theory and what are the non-trivial issues which arise.

For now the considerations apply for zero or finite applied force. In usual diagrammatics, extracting a leg from a vertex corresponds to a derivation. Here this can be done as usual with no ambiguity, provided the corresponding vertex is evaluated at a generic u (e.g. the graphs in Fig II.2). If the vertex is evaluated at $u = 0$ (here and in the following we call them *saturated vertices*) one must go back to a careful application of Wick's rules. Any graph containing such a vertex and which vanishes in the analytic theory is called anomalous. Let us write the series expansion in powers of $|u|$:

$$\Delta(u) = \Delta(0) + \Delta'(0^+)|u| + \frac{1}{2}\Delta''(0^+)u^2 + \dots \ . \quad \text{(II.9)}$$

Wick's rules can then be applied but usually end up in evaluating non-trivial averages of e.g. sign or delta functions.

Let us consider as an example the following 2-loop 1PI diagram (noted e_1 in what follows) which is a correction to the effective action of the form:



$$= \hat{u}_{r\tau}\hat{u}_{r\sigma}\Delta''(u_{r,\tau} - u_{r,\sigma}) \quad \text{(II.10)}$$

$$\times \int_{t_i>0, r_i} R_{r_1-r_2,t_1} R_{r_1-r_2,t_2} R_{r-r_1,t_3} R_{r-r_2,t_4}$$
$$\times \Delta'(u_{r_1,\tau-t_3} - u_{r_1,\tau-t_4-t_1})\Delta'(u_{r_2,\tau-t_4} - u_{r_2,\tau-t_2-t_3}) \ .$$

Here four Wick contractions have been performed, as in any of the other thirty 2-loop diagrams of the form A (studied in the next Section). In an analytic theory performing the local time expansion this would result in a 2-loop correction to $\Delta(u)$ proportional to $\Delta''(u)$ but with a zero coefficient since the Δ' functions are evaluated at zero argument. In the non-analytic theory, inserting the expansion (II.9) yields (upon some change of variables):

$$\mathrm{e}_1 = \Delta'(0^+)^2\Delta''(u)\int_{t_i>0, r_i} R_{r_1,t_1} R_{r_1,t_2} R_{r_3-r_1,t_3} R_{r_3,t_4} F_{r_i,t_i}$$
$$F_{r_i,t_i} = \langle \mathrm{sgn}(X)\mathrm{sgn}(Y)\rangle \quad \text{(II.11)}$$
$$X = u_{r_1,-t_3} - u_{r_1,-t_4-t_1}$$
$$Y = u_{0,-t_4} - u_{0,-t_3-t_2}$$

terms of higher order in (II.9) do not contribute since we are at $T = 0$ and we have exhausted the number of $\hat{u}$ to contract (i.e those terms would yield higher orders in T). The remaining average in (II.11) is evaluated with respect to a Gaussian measure, and can thus be performed. It can be defined by using the $T > 0, v > 0$ Gaussian measure ($u_{xt} \to vt + u_{xt}$) and taking the limit $T \to 0, v \to 0$. The result is a continuous function of v^2/T and its value depends on how the limit is taken.

In the static theory one should take $T \to 0$ at $v = 0$. This yields

$$\langle \mathrm{sgn}(X)\mathrm{sgn}(Y)\rangle = \frac{2}{\pi}\mathrm{asin}(\sigma) \quad \text{(II.12)}$$
$$\sigma = \frac{\langle XY\rangle}{\sqrt{\langle X^2\rangle}\sqrt{\langle Y^2\rangle}}$$

i.e. the result for centered Gaussian variables. Expressing the averages in (II.12) using correlation functions $C_{q,t}$ yields a complicated $T = 0$ expression for e_1. This expression will be discussed in a companion paper on the statics[34]. A list of all anomalous diagrams is presented in Appendix K.

The opposite limit $v \to 0$ at $T = 0$ yields much simpler expressions:

$$\langle \mathrm{sgn}(X)\mathrm{sgn}(Y)\rangle \to \mathrm{sgn}(t_4 + t_1 - t_3)\mathrm{sgn}(t_3 + t_2 - t_4)\ .$$

More generally this procedure corresponds to the substitution: $\Delta^{(n)}(u_{r,t} - u_{r,t'}) \to \Delta^{(n)}(v(t-t'))$ in any ambiguous vertex evaluated at $u = 0$. That this is the correct definition of the theory of the quasi-static depinning as the limit $v = 0^+$ is particularly clear here since it is well known (the no passing property[9,44]) that the $u_{r,t}$ are increasing functions of time in the steady state. Of course it remains to be shown that the procedure actually works and does not produce singular terms such as $\delta(vt)$. It also remains to be shown that it yields a renormalizable continuum theory where all divergences can be removed by the appropriate counter-terms. This is far from trivial and will be achieved below.

Let us comment again on the connections between dynamics and statics. Consider a $T = 0$ dynamical diagram with p connected components evaluated at zero external frequencies. All response functions can be integrated over the times from the leaves towards the root on each connected component. Using the FDT relation this replaces response by correlations and thus exactly reproduces a p replica static diagram except that it is differentiated once with respect to each replica field (the sums over all possible positions of the response field reproduces the derivation chain rule). One simple way to establish this rule is to consider the formal limit $\eta \to 0^+$ (equivalently expansion of $R_{q,\omega}$ in powers of frequency), i.e. formally replace $R_{q,t,t'} \to \delta_{tt'}/q^2$ (keeping track of causality). This reproduces exactly the zero frequencies dynamical diagrams and treats "replicas" as "times".

Thus the p-th derivative of a p replica static diagram gives a set of dynamical diagrams with p connected components. For $p = 2$ this ensures e.g. that the relation $\Delta(u) = -R''(u)$ remains uncorrected to all orders. The flaw in this argument comes from the anomalous diagrams (both in statics and dynamics). In the analytic theory the dynamical diagrams with response fields on a saturated vertex vanish or cancel in pairs. This just expresses that taking a derivative of a static saturated vertex gives zero and the rule still works. But in the non-analytic theory the anomalous diagrams do not vanish and contain an additional time dependence. The above integration of response functions from the leaves to the root cannot be performed for these anomalous diagrams. As a result they can give non-trivial contributions both in statics and dynamics which violate relations such as $\Delta(u) = -R''(u)$, thus allowing to distinguish statics from depinning.

To conclude this Section: The perturbative calculation of the effective action and of the IVF vertices can also be performed in a non-analytic theory. It can be expressed as sums of the same diagrams one writes in the analytic theory, with the same graphical rules to *draw* and generate the diagrams starting from the statics. However the way to compute these diagrams and their *values* is *different* from the analytic theory. The time ordering of vertices comes in a non-trivial way and produces results which can be different at depinning $f = f_c^+$ ($v = 0^+$) and in the statics $f = 0$, as illustrated on the diagram e_1 above. Thus we see the principle mechanism by which the statics and the depinning can yield different field theories, which is a novel result. It remains to perform the actual calculation of these non-analytic diagrams, which is performed in the following sections.

III. RENORMALIZATION PROGRAM

In this section we will compute the effective action to 2-loop order at $T = 0$ for depinning. From the above analysis we know that we only need to compute the 1- and 2-loop corrections to $\Delta(u)$ and η.

A. Corrections to disorder

We start by the corrections to the disorder, first at 1-loop and then at 2-loop order.

1. One loop

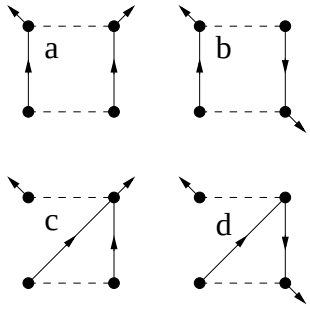


FIG. III.1: 1-loop dynamical diagrams correcting Δ

At leading order, there are four diagrams, depicted on figure III.1. Since diagram (d) is proportional to $\Delta'(u)\Delta'(0)$, it is an odd function of u, and thus does not contribute to the renormalization of Δ. However its repeated counter-term will appear at 2-loop order. Diagram (a) is proportional to $-\Delta(u)\Delta''(u)$, diagram (b) to $-\Delta'(u)^2$ and diagram (c) to $\Delta''(u)\Delta(0)$. All come with a combinatorial factor of $1/2!$ from Taylor-expanding the exponential function, $1/2$ from the action and 4 from combinatorics. Together, they add up to the 1-loop correction to disorder

$$\delta^1\Delta(u) \ = \ \frac{4}{2!\,2}\left[-\Delta'(u)^2 - (\Delta(u) - \Delta(0))\Delta''(u)\right] I_1$$
$$I_1 := \int_q \frac{1}{(q^2+m^2)^2} \qquad \text{(III.1)}$$

with $I_1 = \int_q \mathrm{e}^{-q^2}\Gamma(2 - \frac{d}{2}) = (4\pi)^{-d/2}\Gamma\left(2 - \frac{d}{2}\right)$.

2. Two loops

First, we have to find all diagrams correcting disorder at second order. At $T = 0$ they can be grouped in 3 classes A, B and C for the 3 possible diagrams for unsplitted vertices. Class C does not contribute as is shown in appendix C. We begin our analysis with class A.

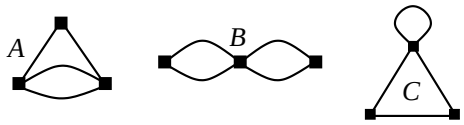


FIG. III.2: The 3 possible classes at second order correcting disorder at $T = 0$. Only classes A and B will contribute.

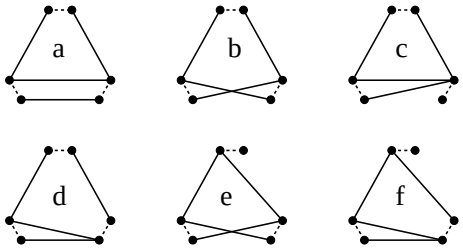


FIG. III.3: Static graphs at 2-loop order in the form of a hat (class A in figure III.2) contributing to two replica terms. Adding a response-field to each connected component leads to the dynamic diagrams of figure III.4.

We now need to write all possible diagrams with splitted vertices of type A. A systematic procedure is to start from all possible static diagrams given in Fig. III.3. This relies on the fact that dynamics and statics are related – recall that in general a dynamic formulation can be used to obtain the renormalization of the statics. As mentionned in the previous Section, to go from the statics to the dynamics, one attaches one response field to a root on each connected component of the diagrams a to f in figure III.3 and orient each component towards the root. The result is presented on figure III.4. The next step is to eliminate all diagrams which yield odd functions of u and thus do not contribute to the renormalized disorder. The list is the following:

$$\begin{aligned} &\mathrm{a}_1 = \mathrm{a}_4 = \mathrm{c}_3 = \mathrm{d}_1 = \mathrm{d}_3 = \mathrm{d}_5 = \mathrm{d}_7 \\ &\quad = \mathrm{e}_2 = \mathrm{e}_3 = \mathrm{f}_1 = \mathrm{f}_3 = \mathrm{f}_4 = \mathrm{f}_5 = 0 \ . \end{aligned} \tag{III.2}$$

Further simplifications come from diagrams, which mutually cancel. Again this uses that $\Delta'(u)$ is an odd function. This gives:

$$\mathrm{c}_2 + \mathrm{c}_5 = \mathrm{d}_2 + \mathrm{d}_4 = \mathrm{d}_6 + \mathrm{d}_8 = 0 \ . \tag{III.3}$$

In addition

$$\mathrm{c}_4 = 0 \ , \tag{III.4}$$

since $\int_{tt'} R_{xt} R_{xt'} \Delta'(t - t') = 0$. This is explained in more details in Appendix K where the list of all anomalous (non-odd) graphs is given together with their expressions in the non-analytic field theory.

Thus, the only non-zero graphs which we have to calculate are a_2, a_3, $\mathrm{b}_1, \ldots, \mathrm{b}_6$, c_1, e_1 and f_2. These calculations are rather cumbersome, due to the appearance of theta-functions of sums or differences of times as a result of the non-analyticity of the theory. The correction to disorder is

$$\delta^2\Delta(u) = \frac{1}{3!}\frac{2}{2^3} 3(2^3) \sum (\mathrm{a}_i + \mathrm{b}_i + ..)$$

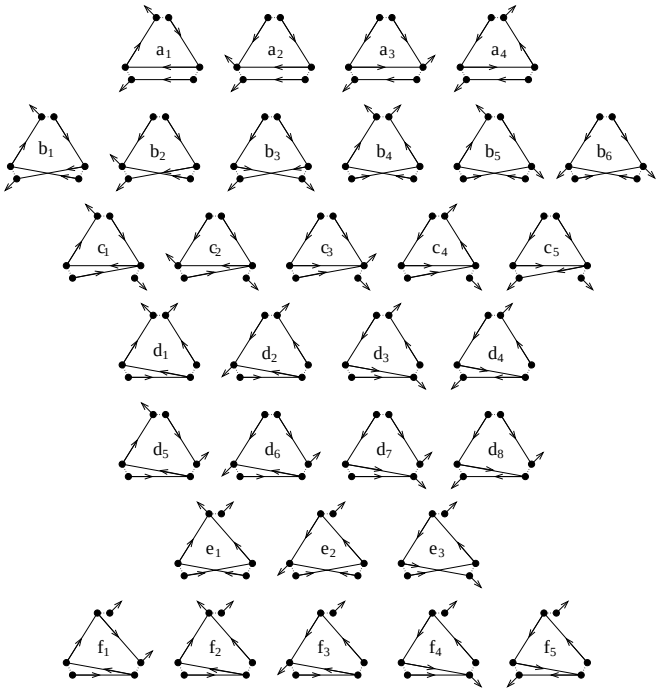


FIG. III.4: Dynamical diagrams at 2-loop order of type A with two external response fields (two connected components) correcting the disorder; derived from the two replica static diagrams of Fig. III.3.

$$= \sum (\mathrm{a}_i + \mathrm{b}_i + ..) \ ,$$

where the combinatorial factors are: $1/3!$ from the Taylor-expansion of the exponential function, $2/2^3$ from the explicit factors of $1/2$ in the interaction, a factor of 3 to chose the vertex at the top of the hat, and a factor of 2 for the possible two choices in each of the vertices. Furthermore below some additional combinatorial factors are given: a factor of 2 for generic graphs and 1 if it has the mirror symmetry with respect to the vertical axis: each diagram symbol (a_i..) denotes the diagram including the symmetry factor.

We recall that we have defined *saturated* vertices as vertices evaluated at $u = 0$ while *unsaturated* vertices still contain u explicitly. Diagrams with response-functions added to unsaturated vertices can be obtained by deriving static diagrams:

$$\begin{aligned} &\mathrm{a}_2 + \mathrm{a}_3 = \text{second derivative of the statics} \\ &\mathrm{b}_1 + \mathrm{b}_2 + \mathrm{b}_3 + \mathrm{b}_4 + \mathrm{b}_5 + \mathrm{b}_6 \\ &\qquad = \text{second derivative of the statics} \end{aligned} \quad . \tag{III.5}$$

The graphs which contain external response-fields on *saturated* vertices cannot be derivatives from static ones. For class A, the hat-diagrams, the only non-zero such graph is c_1.

Explicitly, this reads

$$\mathrm{a}_2 + \mathrm{a}_3 = -\partial_u^2 \left[-R''(0) R'''(u)^2 \right] I_A \ , \tag{III.6}$$

where (see (A.18))

$$I_A := \int \frac{\mathrm{d}^d q_1}{(2\pi)^d} \frac{\mathrm{d}^d q_2}{(2\pi)^d} \frac{1}{q_1^2 + m^2} \frac{1}{q_2^2 + m^2} \frac{1}{((q_1+q_2)^2 + m^2)^2}$$

$$= \left(\frac{1}{2\epsilon^2} + \frac{1}{4\epsilon} + O(\epsilon^2)\right)(\epsilon I_1)^2 \,. \qquad \text{(III.7)}$$

Furthermore, we find

$$\sum_{i=1}^{6} \mathrm{b}_i = -\partial_u^2 \left[R''(u)R'''(u)^2\right] I_A \qquad \text{(III.8)}$$

and

$$\mathrm{c}_1 = 2\Delta'(0^+)^2\Delta''(u) I_A \,. \qquad \text{(III.9)}$$

The diagram e_1 is an explicit example for the appearance of non-trivial sign-functions resulting from the monotonic increase of the displacement. It was already discussed in the previous Section. In the quasi-static depinning limit (II.11) gives (details are given in appendix A):

$$\begin{aligned}\mathrm{e}_1 &= \Delta'(0^+)^2\Delta''(u) \\ &\times \int_{q_1,q_2} \int_{t_1,t_2,t_3,t_4>0} \\ &\mathrm{e}^{-[(q_1^2+m^2)t_1+(q_2^2+m^2)t_2+((q_1+q_2)^2+m^2)(t_3+t_4)} \\ &\mathrm{sgn}(t_1-t_3+t_4)\,\mathrm{sgn}(t_2-t_4+t_3) \,. \qquad \text{(III.10)}\end{aligned}$$

The result of the explicit integration is:

$$\mathrm{e}_1 \;=\; \Delta'(0^+)^2\Delta''(u)\,[I_l - I_A + \text{finite}] \qquad \text{(III.11)}$$

$$\begin{aligned} I_l &:= \int_{q_1,q_2} \frac{1}{(q_1^2+m^2)(q_2^2+m^2)(q_3^2+m^2)(q_1^2+q_3^2+2m^2)} \\ &= \frac{\ln 2}{2\epsilon}(\epsilon I_1)^2 + \text{finite} \,. \qquad \text{(III.12)}\end{aligned}$$

The last diagram f_2 also involves a sign-function and reads:

$$\begin{aligned}\mathrm{f}_2 &= 2\Delta'(0^+)^2\Delta''(u) \int_{q_1,q_2} \int_{t_1,t_2,t_3,t_4>0} \mathrm{sgn}(t_4-t_3-t_2) \times \\ &\times \mathrm{e}^{-[(q_1+q_2)^2+m^2)(t_3+t_4)+(q_1^2+m^2)t_1+(q_2^2+m^2)t_2]} \\ &= -\Delta'(0^+)^2\Delta''(u)\, I_l \,. \qquad \text{(III.13)}\end{aligned}$$

In appendix A we show that (for any given elasticity) the sum of $\mathrm{e}_1 + \mathrm{f}_2$ only involves the integral I_A, and that the combination takes the simpler form

$$\mathrm{e}_1 + \mathrm{f}_2 = -\Delta'(0^+)^2\Delta''(u) I_A \,. \qquad \text{(III.14)}$$

We now turn to graphs of type B (bubble-diagrams).

Again diagrams, which are odd functions of u vanish. These are:

$$\mathrm{h}_1 = \mathrm{h}_2 = \mathrm{i}_1 = \mathrm{j}_1 = \mathrm{k}_2 = \mathrm{k}_3 = \mathrm{l}_2 = \mathrm{l}_3 = \mathrm{l}_4 = 0 \,. \qquad \text{(III.15)}$$

Two other diagram mutually cancel:

$$\mathrm{k}_1 + \mathrm{l}_1 = 0 \,, \qquad \text{(III.16)}$$

as discussed in Appendix K.

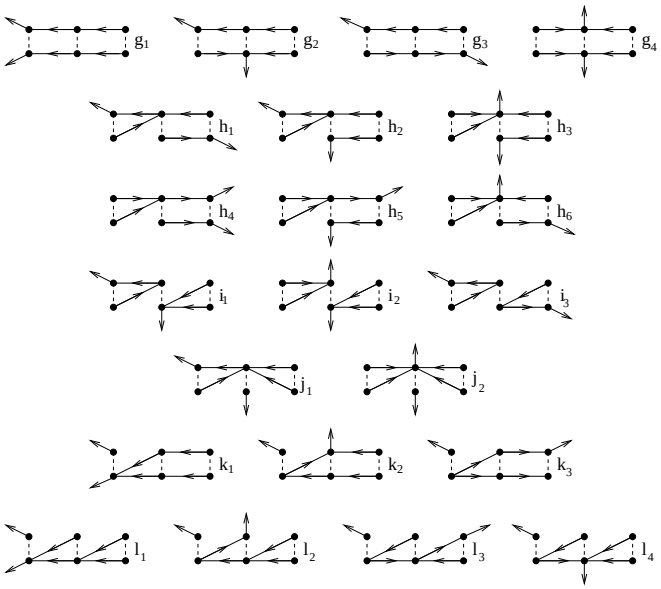


FIG. III.5: 2-loop dynamical diagrams of type B (see figure III.2).

The diagrams that are second derivative of the static have all their response-fields on their unsaturated vertices. These are:

$$\begin{aligned}\mathrm{g}_1 + \mathrm{g}_2 + \mathrm{g}_3 + \mathrm{g}_4 &= \partial_u^2 \left[\frac{1}{2}\Delta(u)^2\Delta''(u)\right] I_1^2 \\ \mathrm{h}_3 + \mathrm{h}_4 + \mathrm{h}_5 + \mathrm{h}_6 &= \partial_u^2 \left[-\Delta(0)\Delta(u)\Delta''(u)\right] I_1^2 \\ \mathrm{i}_2 = \mathrm{j}_2 &= \partial_u^2 \left[\frac{1}{4}\Delta(0)^2\Delta''(u)\right] I_1^2 \,.\end{aligned}$$

The surprise is that i_3, which is not the second derivative of a static diagram, since it has both response fields on saturated vertices, is non-trivial:

$$\mathrm{i}_3 = -\Delta'(0^+)^2\Delta''(u) I_1^2 \,. \qquad \text{(III.17)}$$

To summarize, for the driven problem at $T = 0$ in perturbation of $\Delta \equiv \Delta(u)$, the contributions to the disorder to one and two loops, i.e. the corresponding terms in the effective action $\Gamma[u, \hat{u}]$ are:

$$\delta^1\Delta(u) = -\left[\Delta'(u)^2 + (\Delta(u) - \Delta(0))\Delta''\right] I_1 \qquad \text{(III.18)}$$

$$\begin{aligned}\delta^2\Delta(u) = &\left[(\Delta(u) - \Delta(0))\Delta'(u)^2\right]'' I_A \\ &+\frac{1}{2}\left[(\Delta(u) - \Delta(0))^2\Delta''(u)\right]'' I_1^2 \\ &+\Delta'(0^+)^2\Delta''(u)(I_A - I_1^2) \,. \qquad \text{(III.19)}\end{aligned}$$

Curiously, even though two diagrams contain contributions proportional to $I_l \sim \ln 2$, these contributions cancel in the final result for the corrections to the disorder.

B. Corrections to the friction η

We now calculate the divergent corrections to η, which will require a counter-term proportional to $i\hat{u}\dot{u}$. Let us illustrate



FIG. III.6: 1-loop dynamical diagram correcting the friction.

their calculation at leading order. We start from the first order expansion of the interaction $\mathrm{e}^{-S_{\rm int}}$, which can be written as

$$\int_{t>t',x} i\hat{u}_{xt}\,\Delta(u_{xt}-u_{xt'})\,i\hat{u}_{xt'}\ . \tag{III.20}$$

Contracting one $i\hat{u}_{xt'}$ leads to:

$$\int_{t>t',x} i\hat{u}_{xt}\,\Delta'(u_{xt}-u_{xt'})R_{r=0,t-t'}\ . \tag{III.21}$$

The response function contains a short-time divergence, which we deal with in an operator product expansion. Expanding $\Delta'(u_{xt}-u_{xt'})$ to the necessary order yields

$$\int_{t>t',x} i\hat{u}_{xt}\,\left[\Delta'(0^+)+(u_{xt}-u_{xt'})\Delta''(0^+)+\ldots\right]R_{r=0,t-t'}\ . \tag{III.22}$$

The first term of this expansion, proportional to $\Delta'(0^+)$, is strongly UV-divergent and non-universal and gives the critical force to lowest order in disorder. Since we tune f to be exactly at the depinning threshold we do not need to consider it. The second contribution, proportional to $\Delta''(0^+)$, corrects the friction: due to the short-range singularity in the response-function, we can expand $(u_{xt}-u_{xt'})$ in a Taylor-series, of which only the first term contributes. (III.22) becomes:

$$\int_{t>t',x} i\hat{u}_{xt}\,\left[(t-t')\dot{u}_{xt}+O(t-t')^2\right]\Delta''(0^+)R_{r=0,t-t'}\ . \tag{III.23}$$

The correction to friction at leading order thus is

$$\delta\eta=-\Delta''(0^+)\int_t tR_{r=0,t}\ . \tag{III.24}$$

Here, the response-function is taken at spatial argument 0. In momentum representation, the same expression reads

$$\begin{aligned}\delta\eta&=-\Delta''(0^+)\int_t\int_q tR_{q,t}\\&=-\Delta''(0^+)\int_q t\,\mathrm{e}^{-t(q^2+m^2)}\\&=-\Delta''(0^+)\int_q\frac{1}{(q^2+m^2)^2}\\&=-\Delta''(0^+)\,I_1\end{aligned} \tag{III.25}$$

with the already known integral I_1, equation (III.1).

We now turn to the 2-loop corrections. There are seven contributions, drawn on figure III.7. Their contribution to η is

$$\delta\eta=-\frac{1}{8}\times 4\times 2\,[\mathrm{a}+\mathrm{b}+\mathrm{c}+\mathrm{d}+\mathrm{e}+\mathrm{f}+\mathrm{g}]\ . \tag{III.26}$$

The combinatorial factor is $1/8$ from the interaction, 4 from the time-ordering of the vertices, and an additional factor of 2 for the symmetry of diagrams a, b, e, f and g. Details of the calculation of diagrams a to g are given in appendix D. Grouping diagrams, which partially cancel, we find:

$$\mathrm{a}+\mathrm{g}=-\Delta''(0^+)^2I_1^2 \tag{III.27}$$

$$\mathrm{b}+\mathrm{c}+\mathrm{d}=-\frac{1}{2}\Delta'''(0^+)\Delta'(0^+)I_1^2 \tag{III.28}$$

$$\mathrm{e}=-\Delta'''(0^+)\Delta'(0^+)I_\eta \tag{III.29}$$

$$\mathrm{f}=-2\Delta'''(0^+)\Delta'(0^+)I_A-2\Delta''(0^+)^2I_A \tag{III.30}$$

This involves the non-trivial diagram I_η

$$\begin{aligned}I_\eta&:=\int_{q_1,q_2}\frac{1}{(q_1^2+m^2)(q_2^2+m^2)^2(q_2^2+q_3^2+2m^2)}\\&=\left(\frac{1}{2\epsilon^2}+\frac{1-2\ln 2}{4\epsilon}\right)(\epsilon I_1)^2+\text{finite}\end{aligned} \tag{III.31}$$

calculated in appendix E.

C. Renormalization program to two loops and calculation of counter-terms

1. Renormalization of disorder

Let us now discuss the strategy to renormalize the present theory where the interaction is not a single coupling-constant, but a whole function, the disorder-correlator $\Delta(u)$. We denote by Δ_0 the bare disorder – this is the object in which perturbation theory is carried out – i.e. one consider the bare action (II.2) with $\Delta\to\Delta_0$. We denote here by Δ the renormalized dimensionless disorder i.e. the corresponding term in the effective action $\Gamma[u,\hat{u}]$ is $m^\epsilon\Delta$.

We define the dimensionless bilinear 1-loop and trilinear 2-loop symmetric functions (see (III.18) and (III.19)) such that:

$$\delta^{(1)}(\Delta,\Delta)=m^\epsilon\delta^1\Delta \tag{III.32}$$

$$\delta^{(2)}(\Delta,\Delta,\Delta)=m^\epsilon\delta^2\Delta \tag{III.33}$$

thus extended to non-equal argument using $f(x,y):=\frac{1}{2}\left[f(x+y,x+y)-f(x,x)-f(y,y)\right]$ and a similar expression for the trilinear function. Whenever possible we will use

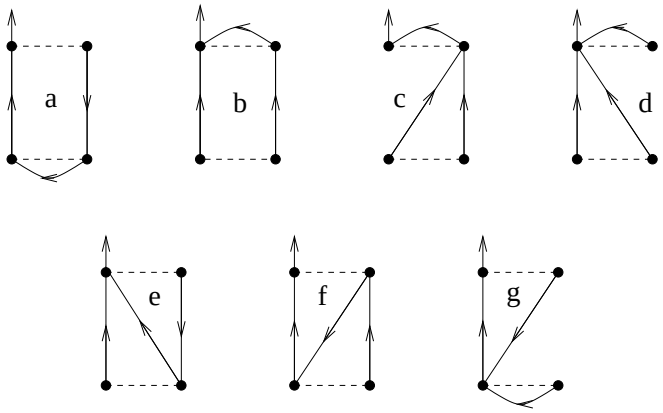


FIG. III.7: 2-loop dynamical diagrams correcting the friction. They all have multiplicity 8 except (c) and (d) which have multiplicity 4.

the shorthand notation $\delta^{(1)}(\Delta) = \delta^{(1)}(\Delta, \Delta)$ and $\delta^{(2)}(\Delta) = \delta^{(2)}(\Delta, \Delta, \Delta)$. The expression of Δ obtained perturbatively in powers of Δ_0 at 2-loop order reads:

$$\Delta = m^{-\epsilon}\Delta_0 + \delta^{(1)}(m^{-\epsilon}\Delta_0) + \delta^{(2)}(m^{-\epsilon}\Delta_0) + O(\Delta_0^4) \; . \tag{III.34}$$

It contains terms of order $1/\epsilon$ and $1/\epsilon^2$. This is sufficient to calculate the RG-functions at this order (In principle, one has to keep the finite part of the 1-loop terms, but we will work in a scheme, where these terms are exactly 0, by normalizing all diagrams by the 1-loop diagram). Inverting this formula yields:

$$\Delta_0 = m^{\epsilon}\Big[\Delta - \delta^{(1)}(\Delta) - \delta^{(2)}(\Delta) + \delta^{(1,1)}(\Delta) + \dots\Big] \; , \tag{III.35}$$

where $\delta^{(1,1)}(\Delta)$ is the 1-loop repeated counter-term:

$$\delta^{(1,1)}(\Delta) = 2\delta^{(1)}(\Delta, \delta^{(1)}(\Delta, \Delta)) \; . \tag{III.36}$$

The β-function is by definition the derivative of Δ at fixed Δ_0. It reads:

$$-m\partial_m \Delta\big|_{\Delta_0} = \epsilon\Big[m^{-\epsilon}\Delta_0 + 2\delta^{(1)}(m^{-\epsilon}\Delta_0) + 3\delta^{(2)}(m^{-\epsilon}\Delta_0) + \dots\Big] \tag{III.37}$$

Using the inversion formula (III.35), the β-function can be written in terms of the renormalized disorder Δ:

$$-m\partial_m \Delta\big|_{\Delta_0} = \epsilon\Big[\Delta + \delta^{(1)}(\Delta) + 2\delta^{(2)}(\Delta) - \delta^{(1,1)}(\Delta) + \dots\Big] \tag{III.38}$$

In order to proceed, let us calculate the repeated 1-loop counter-term $\delta^{1,1}(\Delta)$. We start from the 1-loop counter-term (III.18), which has the bilinear form

$$\delta^{(1)}(f,g) = -\frac{1}{2}\Big[2f'(u)g'(u) + (f(u) - f(0))g''(u) + (g(u) - g(0))f''(u)\Big]\tilde{I}_1 \tag{III.39}$$

with the dimensionless integral $\tilde{I}_1 := I_1\big|_{m=1}$; we will use the same convention for $\tilde{I}_A := I_A\big|_{m=1}$. Thus $\delta^{1,1}(\Delta)$ reads

$$\begin{aligned}\delta^{(1,1)}(\Delta(u)) &= 2\delta^{(1)}\Big(\Delta, \delta^{(1)}(\Delta)\Big) \\ &= \Big[(\Delta(u) - \Delta(0))^2\Delta''(u) \\ &\quad + (\Delta'(u)^2 - \Delta'(0)^2)(\Delta(u) - \Delta(0))\Big]''\tilde{I}_1^2\end{aligned} \tag{III.40}$$

Note that this counter-term is non-ambiguos for $u \to 0$. Finally, as discussed at the end of the previous section at any point we can rescale the fields u by m^{ζ}. This amounts to write the β-function for the function $\tilde{\Delta}(u) = m^{-2\zeta}\Delta(um^{\zeta})$ which will be implicit in the following (in addition we will drop the tilde superscript).

The 2-loop β-function (III.38) then becomes with the help of (III.40)

$$\begin{aligned}-m\partial_m \Delta(u) &= (\epsilon - 2\zeta)\Delta(u) + \zeta u\Delta'(u) \\ &\quad - \frac{1}{2}\left[(\Delta(u) - \Delta(0))^2\right]''(\epsilon\tilde{I}_1) \\ &\quad + \left[(\Delta(u) - \Delta(0))\Delta'(u)^2\right]''\epsilon\Big(2\tilde{I}_A - \tilde{I}_1^2\Big) \\ &\quad + \Delta'(0^+)^2\Delta''(u)\,\epsilon\Big(2\tilde{I}_A - \tilde{I}_1^2\Big) \; .\end{aligned} \tag{III.41}$$

One of our main results is now apparent: the $1/\epsilon^2$-terms cancel in the corrections to disorder. If it had not been the case it would lead to a term of order $1/\epsilon$ in the β-function and thus to non-renormalizability. Thus the β-function is finite to two loops a hallmark of a renormalizable theory. Note that this happened in a rather non-trivial way since it required a consistent evaluation of all anomalous non-analytic diagrams. Furthermore the precise type of cancellation is unusual: usually the 2-loop bubble diagrams of type B are simply the square of the 1-loop ones. Here the easily missed and non-trivial bubble diagram i_3 was crucial in achieving the above cancellation.

In order to simplify notations and further calculations, we absorb a factor of $\epsilon\tilde{I}_1$ in the definition of the renormalized disorder (or equivalently in the normalization of momentum or space integrals). With this, the β-function takes the simple form:

$$\begin{aligned}-m\partial_m \Delta(u) &= (\epsilon - 2\zeta)\Delta(u) + \zeta u\Delta'(u) \\ &\quad - \frac{1}{2}\left[(\Delta(u) - \Delta(0))^2\right]'' \\ &\quad + \frac{1}{2}\left[(\Delta(u) - \Delta(0))\Delta'(u)^2\right]'' \\ &\quad + \frac{1}{2}\Delta'(0^+)^2\Delta''(u) \; .\end{aligned} \tag{III.42}$$

Note several interesting features of this 2-loop β-function. First it contains a non-trivial so called "anomalous term" (the last one) which is absent in an analytic theory. Second, it can be shown to exhibit irreversibility, precisely due to this term. Although, surprisingly, it can be formally be integrated twice over u the resulting flow equation for the double primitive of $\Delta(u)$ does not, however, have the required property for the flow of a potential function, i.e. a second cumulant of the random potential in the static. This will be shown in details in the next Section IV where we find that the fixed points of the above equation are manifestly non-potential. In Ref.[33] we have obtained the corresponding beta function for $R(u)$ in the statics. The corresponding force force correlator $\Delta_{\rm stat}(u) = -R''(u)$ obeys the same equation than (III.42) but with the opposite sign for the anomalous term! This shows that statics and depinning are indeed two different theories at two loops.

2. Renormalization of friction and dynamical exponent z

In section III B, we have calculated the effective (renormalized) friction coefficient η_R as a function of the bare one η_0 and the bare disorder Δ_0:

$$\eta_R = \eta_0 Z[m^{-\epsilon}\Delta_0]^{-1} \; . \tag{III.43}$$

This identifies the renormalization group Z-factor as

$$Z^{-1}[m^{-\epsilon}\Delta_0] = 1 - \Delta_0''(0^+)I_1 + \left[\Delta_0''(0^+)\right]^2\left[I_1^2 + 2I_A\right] + \Delta_0'''(0^+)\Delta_0'(0^+)\left[\frac{1}{2}I_1^2 + 2I_A + I_\eta\right] . \quad \text{(III.44)}$$

The dynamical exponent z is then given by

$$z = 2 + m\frac{\mathrm{d}}{\mathrm{d}m}\ln Z(m^{-\epsilon}\Delta_0) . \quad \text{(III.45)}$$

Equation (III.44) yields

$$\ln Z^{-1} = - \Delta_0''(0^+)I_1 + \Delta_0''(0^+)^2\left[\frac{1}{2}I_1^2 + 2I_A\right] + \Delta_0'''(0^+)\Delta_0'(0^+)\left[\frac{1}{2}I_1^2 + 2I_A + I_\eta\right] \quad \text{(III.46)}$$

and thus (remind that $I_1 \sim m^{-\epsilon}$ and $I_A \sim I_\eta \sim m^{-2\epsilon}$)

$$m\frac{\mathrm{d}}{\mathrm{d}m}\ln Z^{-1} = \Delta_0''(0^+)(\epsilon I_1) - \Delta_0''(0^+)^2\,\epsilon\big(I_1^2 + 4I_A\big) + \Delta_0'''(0^+)\Delta_0'(0^+)\,\epsilon\big(I_1^2 + 4I_A + 2I_\eta\big) \quad \text{(III.47)}$$

We now have to express Δ_0 in terms of the renormalized disorder Δ using (III.35). For the second-order terms, this relation is simply $\Delta_0 = m^\epsilon\Delta$. The non-trivial term is $\Delta''(0^+)$. Using (III.18), derived twice at 0^+, we get (with the factor of (ϵI_1) absorbed into the renormalized disorder

$$\Delta_0''(0^+) = (\epsilon I_1)^{-1}\times \times\left[\Big(\Delta''(0^+) + \tilde{I}_1(4\Delta'''(0^+)\Delta'(0^+) + 3\Delta''(0^+)^2\Big)\right] \quad \text{(III.48)}$$

Putting everything together, the result is

$$m\frac{\mathrm{d}}{\mathrm{d}m}\ln Z^{-1} = \Delta''(0^+) + \epsilon\left(\frac{2}{\epsilon^2} - \frac{4I_A}{(\epsilon I_1)^2}\right)\Delta''(0^+)^2 + \epsilon\left(\frac{3}{\epsilon^2} - \frac{4I_A}{(\epsilon I_1^2)} - \frac{2I_\eta}{(\epsilon I_1^2)}\right)\Delta'''(0^+)\Delta'(0^+) \quad \text{(III.49)}$$

Again there is a non-trivial cancellation of the $1/\epsilon$ terms, another manifestation of the renormalizability of the theory. Inserting the values of the integrals I_A and I_η, the dynamical exponent z becomes:

$$z = 2 - \Delta''(0^+) + \Delta''(0^+)^2 + \Delta'''(0^+)\Delta'(0^+)\left[\frac{3}{2} - \ln 2\right] . \quad \text{(III.50)}$$

D. Finiteness and scaling form of correlations and response functions

To complete the 2-loop renormalizability program one must check that all correlation and response functions are rendered finite by the above counter-terms. In a more conventional theory that would be more or less automatic. Here however there are additional subtleties. The disorder counter-term is a full function and is purely static. This counter-term, and its associated FRG equation (III.42) cannot be read at $u = 0$ because of the non-analytic action (this point is further explained in Appendix K). Indeed, this equation and the cancellation of divergent parts was established only for $u \neq 0$. It remains to be checked that irreducible vertex functions which are $u = 0$ quantities are also rendered finite by the above static $u \neq 0$ counter-terms.

We first examine the two point correlation function. We will first show that it is *purely static*. Then, in appendix K we show that it is finite and perform its calculation in the renormalized theory. One has

$$\langle u_{q\omega}u_{-q-\omega}\rangle = \mathcal{R}_{q\omega}\mathcal{R}_{-q,-\omega}\Gamma_{i\hat{u}i\hat{u}}(q\omega) , \quad \text{(III.51)}$$

where $\mathcal{R}_{q\omega}$ is the (exact) response function. We will thus only compute $\Gamma_{i\hat{u}i\hat{u}}(qt)$ (in time variable). The 1-loop counter-term for η is absent in this $\mathcal{O}(\Delta^2)$ calculation of the proper vertex but it enters the calculation of $\langle u_{q\omega}u_{-q-\omega}\rangle$ (it dresses the external legs $R_{q\omega}$ into $\mathcal{R}_{q\omega}$). In fact since we find that $\Gamma_{i\hat{u}i\hat{u}}(qt)$ is static (independent of t) we will need only the exact response at zero frequency, which is the bare one because of STS.

To one loop, the proper vertex $\Gamma_{i\hat{u}i\hat{u}}(q\omega)$ is the sum of the graphs a, b, c and d of Fig. III.6 evaluated at finite frequency and momentum, so we write $\Gamma_{i\hat{u}i\hat{u}}(q\omega) = \mathrm{a} + \mathrm{b} + \mathrm{c} + \mathrm{d}$. The sum $\mathrm{a} + \mathrm{b}$ yields after two Wick contractions and short distance expansion a term proportional to

$$\int_{k,t_i} i\hat{u}_t i\hat{u}_{t'}\Delta''(u_t - u_{t'})\Delta(u_{t_1} - u_{t_2}) \times(R_{k,t'-t_2} - R_{k,t-t_2})(R_{k,t-t_1} - R_{k,t'-t_1}) , \quad \text{(III.52)}$$

where we have kept all times explicitly to resolve any ambiguity. Expressing Δ in a series as in (II.9), the lowest order term is purely static (since one can integrate freely over t_1, t_2), and proportional to $\Delta''(0+)\Delta(0)\int_k k^{-4}$, but vanishes from the cancellation between graphs a and b. As explained in detail in Appendix K there can be a priori another contribution coming from $2\Delta'(0^+)^2\delta(u)u$ in the expansion of $\Delta''\Delta$. It produces a term $\delta(v(t-t'))v|t_1 - t_2|$ which vanishes when multiplied with the above response function combination (since it vanishes at $t = t'$).

Thus the only contribution comes from $\mathrm{c} + \mathrm{d}$. There the Δ' yields sign functions and there are no ambiguities. One finds:

$$\begin{aligned}\mathrm{d} &= -2\Delta'(0+)^2\int_{\tau_1,\tau_2>0}[\mathrm{sgn}(t-\tau_2) + \mathrm{sgn}(-t-\tau_2)] \\ &\quad\times\int_k \mathrm{e}^{-k^2\tau_2}\mathrm{e}^{-(k+q)^2\tau_1} \\ &= -2\Delta'(0+)^2\int_k \frac{1}{k^2(k+q)^2}\mathrm{e}^{-k^2|t|/\eta}\end{aligned}$$

$$\begin{aligned}\mathrm{b} &= \Delta'(0+)^2 \int_{\tau_1,\tau_2>0} \mathrm{sgn}(\tau_1 + t/\eta)\,\mathrm{sgn}(\tau_2 - t/\eta) \\ &\quad \times \int_k \mathrm{e}^{-k^2\tau_2}\mathrm{e}^{-(k+q)^2\tau_1} \\ &= \Delta'(0+)^2 \int_k \frac{1}{k^2(k+q)^2}\left(2\mathrm{e}^{-k^2|t|/\eta} - 1\right) ,\end{aligned}$$

where we have accounted for the extra combinatoric factor of 2 for graph d and used

$$\int_{\tau>0} \mathrm{e}^{-q^2\tau}\mathrm{sgn}(\tau - t) = \frac{1}{q^2}\left(\theta(t)(2\mathrm{e}^{-q^2 t} - 1) + \theta(-t)\right) . \tag{III.53}$$

We thus find that although each graph is time dependent, this time-dependence cancels in the sum. Thus we find a static result:

$$\Gamma_{i\hat{u}i\hat{u}}(q\omega) = \delta(\omega)\left[\Delta(0) - \Delta'(0+)^2 \int_k \frac{1}{k^2(k+q)^2}\right] . \tag{III.54}$$

The static 1-loop counter-term should thus be sufficient to cancel the divergence of (III.54). This is further analyzed in Appendix J where the full correlation-function is computed.

We have thus found the commutation $\Gamma_{i\hat{u}i\hat{u}}(u = 0, q) = \Gamma_{i\hat{u}i\hat{u}}(u = 0^+, q)$. Note that if all correlation functions are purely static, i.e. strictly time-independent, it implies the commutation of the limits. Then it also implies the finiteness since these static divergences have been removed. We have not pushed the analysis further but we found a simple argument which indicates that all correlations are indeed static. We found that the time dependence in diagrams cancels by subsets, noting[63] that graphs can be grouped in subsets (e.g. pairs ac, bd, ef in Fig. III.3) which vanish by shifting the endpoint of an internal line within a splitted vertex.

Finally, let us note that our result that correlations at the quasi static depinning are purely *static* for $v = 0^+$ is at variance with previous works[19,20]. Thus the only functions where the dynamical exponent comes in are response function.

E. Long range elasticity

As was discussed in the Introduction there are physical systems where the elastic energy does not scale with the square of the wave-vector q as $E_{\mathrm{elastic}} \sim q^2$ but as $E_{\mathrm{elastic}} \sim q^\alpha$. In this situation, the upper critical dimension is $d_c = 2\alpha$ and we define:

$$\epsilon := 2\alpha - d . \tag{III.55}$$

The most interesting case, a priori relevant to model wetting or crack-front propagation is $\alpha = 1$, thus $d_c = 2$.

In order to proceed, we have again to specify a cut-off procedure. For calculational convenience, we choose the elastic energy to be

$$E_{\mathrm{elastic}} \sim (q^2 + m^2)^{\frac{\alpha}{2}} . \tag{III.56}$$

This changes the response-function to

$$R_{q,t} = \Theta(t)\,\mathrm{e}^{-(q^2+m^2)^{\frac{\alpha}{2}}t} . \tag{III.57}$$

Since contributions proportional to I_l, see (A.26), cancel, the only integrals which appear in the β-function are:

$$I_1^{(\alpha)} = \int_q \frac{1}{(q^2+m^2)^\alpha} = m^{-\epsilon}\frac{\Gamma(\epsilon/2)}{\Gamma(\alpha)}\int_q \mathrm{e}^{-q^2} \tag{III.58}$$

$$I_A^{(\alpha)} = \int_{q_1,q_2} \frac{1}{(q_1^2+m^2)^{\frac{\alpha}{2}}(q_2^2+m^2)^\alpha((q_1+q_2)^2+m^2)^{\frac{\alpha}{2}}} \tag{III.59}$$

The important combination is again $2I_A^{(\alpha)} - (I_1^{(\alpha)})^2$. One finds (see appendix F)

$$\begin{aligned}X^{(\alpha)} &:= \frac{2\,\epsilon(2I_A^{(\alpha)} - (I_1^{(\alpha)})^2)}{(\epsilon I_1^{(\alpha)})^2} \\ &= \int_0^1 \frac{\mathrm{d}t}{t}\,\frac{1 + t^{\frac{\alpha}{2}} - (1+t)^{\frac{\alpha}{2}}}{(1+t)^{\frac{\alpha}{2}}} + \frac{\Gamma'(\alpha)}{\Gamma(\alpha)} - \frac{\Gamma'(\frac{\alpha}{2})}{\Gamma(\frac{\alpha}{2})} \\ &\quad + O(\epsilon) .\end{aligned} \tag{III.60}$$

Since this term is finite, the β-function is finite; this is of course necessary for the theory to be renormalizable. For the cases of interest $\alpha = 1$ and $\alpha = 2$, we find

$$X^{(2)} = 1 \tag{III.61}$$

$$X^{(1)} = 4\ln 2 . \tag{III.62}$$

Since there is only one non-trivial diagram at second order, all 2-loop terms in the β-function get multiplied by $X^{(\alpha)}$:

$$\begin{aligned}-m\partial_m\Delta(u) &= (\epsilon - 2\zeta)\Delta(u) + \zeta u\Delta'(u) \\ &\quad -\frac{1}{2}\left[(\Delta(u) - \Delta(0))^2\right]'' \\ &\quad +\frac{X^{(\alpha)}}{2}\left[(\Delta(u) - \Delta(0))\Delta'(u)^2\right]'' \\ &\quad +\frac{X^{(\alpha)}}{2}\Delta'(0^+)^2\Delta''(u) .\end{aligned} \tag{III.63}$$

The diagrams involved in the dynamics also change. Besides $I_1^{(1)}$ and $I_A^{(1)}$ given above we need

$$\begin{aligned}I_\eta^{(1)} &:= \int_{q_1,q_2} \frac{1}{(q_1^2+m^2)^{\frac{1}{2}}\,(q_2^2+m^2)\,[(q_2^2+m^2)^{\frac{1}{2}} + (q_3^2+m^2)^{\frac{1}{2}}]} \\ &= \left(\frac{1}{2\epsilon^2} + \frac{\ln 2 - \frac{\pi}{4}}{\epsilon}\right)\left(\epsilon I_1^{(1)}\right)^2 + \text{finite}\end{aligned} \tag{III.64}$$

calculated in appendix G.

Starting from (III.49), the dynamical exponent z is then in straightforward generalization of (III.50) given by

$$z = \alpha - \Delta''(0^+) + X^{(\alpha)}\Delta''(0^+)^2 + Y^{(\alpha)}\Delta'''(0^+)\Delta'(0^+) \tag{III.65}$$

with $X^{(\alpha)}$ given above and

$$Y^{(\alpha)} = X^{(\alpha)} + \frac{2I_\eta^{(\alpha)} - \left(I_1^{(\alpha)}\right)^2}{\epsilon\left(I_1^{(\alpha)}\right)^2} \tag{III.66}$$

$$Y^{(1)} = 6\ln 2 - \frac{\pi}{2} \tag{III.67}$$

$$Y^{(2)} = \frac{3}{2} - \ln 2 . \tag{III.68}$$

The case $\alpha = 2$ reproduces (III.50). Since both $X^{(1)}$ and $Y^{(1)}$ are finite, we have checked that also in the case of long-range elasticity the theory is renormalizable at second order.

IV. ANALYSIS OF FIXED POINTS AND PHYSICAL RESULTS

The FRG-equation derived above describes several different physical situations: periodic systems (such as charge density waves) where the disorder correlator is periodic and non-periodic systems (such as a a domain-wall in a magnet). Within the latter, SR (random bond) and LR (random field) disorder must a priori be distinguished. In our analysis of the FRG-equations, we have to study these situations separately.

Before we do so, let us mention an important property, valid under all conditions: If $\Delta(u)$ is solution of (III.63), then

$$\tilde{\Delta}(u) := \kappa^2 \Delta(u/\kappa) \tag{IV.1}$$

is also a solution. We can use this property to fix $\Delta(0)$ in the case of non-periodic disorder. (For periodic disorder the solution is unique, since the period is fixed.)

A. Non-periodic systems

We now start our analysis with non-periodic systems, either with random field disorder or any correlator decreasing faster than RF. Let us first recall that at the level of the *bare* model the static RF obeys $R(u) \sim -\sigma|u|$ at large $|u|$ and thus $\int_0^\infty du \Delta(u) = R'(0^+) - R'(\infty) = -\sigma$ (σ is the amplitude of the random field) while RB or any correlator decaying faster than RF satisfies $\int \Delta = 0$.

Let us first integrate the disorder flow equation (III.63) from $u = 0^+$ to $u = +\infty$. We obtain

$$-m\partial_m \int_0^\infty \Delta(u)\, \mathrm{d}u = (\epsilon - 3\zeta) \int_0^\infty \Delta(u)\, \mathrm{d}u - X^{(\alpha)} \Delta'(0^+)^3 \,. \tag{IV.2}$$

The only assumption that we have made here is that $u\Delta(u)$ goes to zero at $u = +\infty$, which is the case both for RB and RF.

Let us first recall the 1-loop analysis, where in the FRG equation there is no distinction between statics and depinning. The last term in (IV.2) is then absent. Thus one finds either fixed points with $\int \Delta = \sigma > 0$ with $\zeta = \epsilon/3$, the RF universality class, or others with $\int \Delta = 0$ for $\zeta < \epsilon/3$ which corresponds to disorder with shorter range correlations than than RF. This includes the RB fixed point with exponentially decaying correlator and $\zeta_{RB} = 0.208\epsilon$. It also includes a continuous family of intermediate power law fixed points[32,36] with decay at large u as $\Delta(u) = -R''(u) \sim (\alpha - 2)(\alpha - 1)u^{-\alpha}$ with $\alpha^* > \alpha > 1$. These have $\zeta(\alpha) = \epsilon/(2+\alpha)$ (from solving the linear part of the FRG equation) and $\zeta(\alpha^*) = \zeta_{RB}$.

The last term in (IV.2) shows that things work differently to two loops at depinning. the condition $\int \Delta = 0$ is no longer possible at the fixed point. Starting from RB one develops a positive value for $\int \Delta$, i.e. a random field component. The natural conclusion is then that all correlations shorter range than RF flow to the RF universality class[76]. Furthermore the fixed point condition (III.63) equals 0 implies a unique well defined value for ζ identical for all ranges shorter than RF (including RB). This value takes the form:

$$\zeta = \frac{\epsilon}{3} - \frac{X^{(\alpha)} \Delta'(0^+)^3}{3 \int_0^\infty \Delta} = \frac{\epsilon}{3} + \zeta_2 \epsilon^2 + O(\epsilon^3) \,, \tag{IV.3}$$

where $\zeta_2 > 0$ can be obtained from the knowledge of the 1-loop fixed point $\Delta \sim O(\epsilon)$ only.

Before we compute ζ_2 and obtain the depinning fixed point to two loop, let us note that in the static case[33] the last term in (III.63) has the opposite sign and, integrating over u one finds that there is thus no term proportional to $\Delta'(0^+)$ in (IV.2). Thus for the RF disorder $0 < \int \Delta < +\infty$ one can again conclude that

$$\zeta_{\rm eq}^{\rm RF} = \frac{\epsilon}{3} \tag{IV.4}$$

to (at least) second order. In fact, as discussed in[33] this is expected to be exact to all orders due to the potentiality requirement of the static FRG equation, which also implies that $\int \Delta = 0$ holds to all orders at the static RB fixed point. The corresponding value for $\zeta_{\rm eq}^{\rm RB}$ is given to order ϵ^2 in[33].

We now want to find the fixed-point function of equation (III.63). Using the reparametrization-invariance (IV.1), we set (with the factors $1/3$ and $1/18$ chosen for later convenience)

$$\Delta(u) = \frac{\epsilon}{3} y_1(u) + \frac{\epsilon^2}{18} y_2(u) + O(\epsilon^3) \tag{IV.5}$$

$$y_1(0) = 1 \tag{IV.6}$$

$$y_2(0) = 0 \,, \tag{IV.7}$$

where $y_1(u)$ is the 1-loop fixed point function for the RF case. It was obtained in Ref.[22] and further studied in Ref.[28]. Let us recall its properties. To lowest order in ϵ the 1-loop β-function (III.63) reads:

$$\frac{\epsilon}{3}\Delta(u) + \frac{\epsilon}{3} u \Delta'(u) - \frac{1}{2}\Big[(\Delta(u) - \Delta(0))^2\Big]'' = 0 \tag{IV.8}$$

inserting (IV.5) the function $y_1(u)$ must satisfy:

$$[u y_1(u)]' = \frac{1}{2}\Big[(y_1(u) - y_1(0))^2\Big]'' \,, \tag{IV.9}$$

which can be first integrated to

$$u y_1(u) = (y_1(u) - 1)\, y_1'(u) \,, \tag{IV.10}$$

using (IV.6) in the last line. A second integration with the boundary conditions implied by (IV.6) yields:

$$y_1(u) - \ln y_1(u) = 1 + \frac{1}{2}u^2 \,. \tag{IV.11}$$

The derivatives of $y_1(u)$ at $u = 0$ will be needed below. Deriving (IV.10) successively w.r.t. u, we find

$$y_1(0) = 1 \,, \qquad y_1'(0^+) = -1$$
$$y_1''(0^+) = \frac{2}{3} \,, \qquad y_1'''(0^+) = -\frac{1}{6} \,. \tag{IV.12}$$

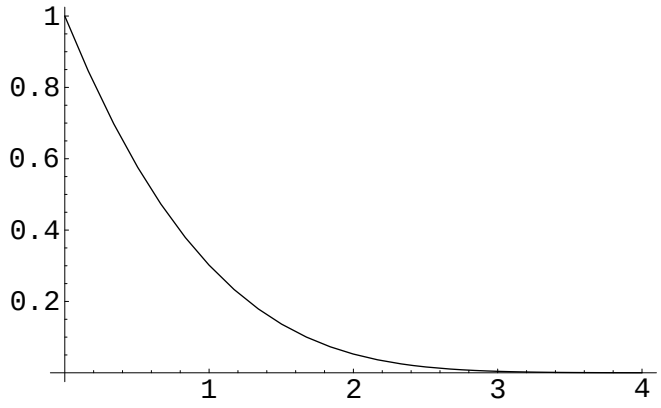


FIG. IV.1: The fixed-point function $y_1(u)$ at 1-loop order for non-periodic disorder.

We have also determined the fixed-point function at second order $y_2(u)$, which is given in appendix H.

In order to extract ζ from (IV.2), we need

$$\sqrt{2}\gamma = \int_0^\infty y_1(u)\,\mathrm{d}u\,, \tag{IV.13}$$

which was computed in Ref.[28]. The method is to convert (IV.13) into an integral over $y := y_1$:

$$\begin{aligned}\int_0^\infty y\,\mathrm{d}u &= -\int_0^1 y\,\frac{\mathrm{d}u}{\mathrm{d}y}\,\mathrm{d}y = -\int_0^1 \frac{y}{y'}\,\mathrm{d}y \\ &= -\int_0^1 \mathrm{d}y\,\frac{y-1}{\sqrt{2}\sqrt{y-\ln y-1}}\,,\end{aligned} \tag{IV.14}$$

where in the last equality (IV.11) has been used. Integrating by parts, this yields

$$\gamma = \int_0^1 \mathrm{d}y\,\sqrt{y-\ln y-1} \approx 0.5482228893\ldots \tag{IV.15}$$

Combining the definition of $\Delta(u)$ in (IV.5) with (IV.12) and (IV.15), we find

$$\zeta_2 = \frac{X^{(\alpha)}}{27\sqrt{2}\gamma} \tag{IV.16}$$

and thus for ζ

$$\zeta = \frac{\epsilon}{3} + \frac{X^{(\alpha)}\epsilon^2}{27\sqrt{2}\gamma} + O(\epsilon^3)\,. \tag{IV.17}$$

This result violates the conjecture of[21], that $\zeta = \frac{\epsilon}{3}$ to all orders in ϵ. To compare (IV.17) with simulations, we have to specify to the cases of interest: First, for short-range elasticity, i.e. $\alpha = 2$, we find

$$\zeta = \frac{\epsilon}{3}\left(1 + \frac{\epsilon}{9\sqrt{2}\gamma}\right) = \frac{\epsilon}{3}\Big(1 + 0.143313\,\epsilon\Big)\,. \tag{IV.18}$$

Our results are in excellent agreement with the numerical simulations, see figure IV.2. For long-range elasticity, i.e. $\alpha = 1$, equation (IV.17) reads

exponent	dim	1-loop	2-loop	estimate	simulation
	$d=3$	0.33	0.38	0.38±0.02	0.34±0.01[19,20]
ζ	$d=2$	0.67	0.86	0.82±0.1	0.75±0.02[51]
	$d=1$	1.00	1.43	1.2±0.2	1.25±0.01[64] 1.25±0.05[51]
	$d=3$	1.78	1.73	1.74 ±0.02	1.75±0.15[19,20]
z	$d=2$	1.56	1.38	1.45±0.15	1.56±0.06[51]
	$d=1$	1.33	0.94	1.35±0.2	1.42±0.04[51] 1.54±0.05[64]
	$d=3$	0.89	0.85	0.84±0.01	0.84±0.02[19,20]
β	$d=2$	0.78	0.62	0.53±0.15	0.65±0.05[51] 0.64±0.02[19,20] 0.66±0.04[52]
	$d=1$	0.67	0.31	0.2±0.2	0.35±0.04[53] 0.4 ± 0.05[64] 0.25±0.03[51]
	$d=3$	0.58	0.61	0.62±0.01	
ν	$d=2$	0.67	0.77	0.85±0.1	0.77±0.04[52]
	$d=1$	0.75	0.98	1.25±0.3	1±0.05[53] 1.1±0.1[64]

FIG. IV.2: Depinning exponents, $\alpha = 2$. First column: Exponents obtained by setting $\epsilon = 1$ in the 1-loop result. Second column: Exponents obtained by setting $\epsilon = 1$ in the two-loop result. Third column: Conservative estimates based on three Padé estimates, scaling relations and common sense. Fourth column: Results of numerical simulations obtained directly without using scaling relations.

$$\zeta = \frac{\epsilon}{3}\left(1 + \frac{4\ln 2}{9\sqrt{2}\gamma}\epsilon\right) = \frac{\epsilon}{3}\Big(1 + 0.39735\,\epsilon\Big)\,. \tag{IV.19}$$

This is in reasonable agreement with simulations, as shown on figure IV.3.

We now turn to the calculation of the dynamical exponent z. As can be seen from the general result of equation (III.65), we need $\Delta'(0^+)$, $\Delta''(0^+)$ and $\Delta'''(0^+)$ at leading order, which can be inferred from (IV.5) and (IV.12). We further need $\Delta''(0)$ at second order. Expanding (III.63) to order ϵ^3, and Taylor-expanding to second order in u, we can solve for $y_2''(0)$, which yields

$$\Delta''(0) = \frac{\epsilon}{3}y_1''(0) + \frac{\epsilon}{18}y_2''(0) \tag{IV.20}$$

exponents	one loop	two loop	estimate	simulation
ζ	0.33	0.47	0.5 ± 0.1	0.390 ± 0.002[45]
z	0.78	0.66	0.7 ± 0.1	0.74 ± 0.03[65]
β	0.78	0.59	0.4 ± 0.2	???
ν	1.33	1.58	$2. \pm 0.4$	???

FIG. IV.3: Depinning exponents, $\alpha = 1$. First column: Exponents obtained by setting $\epsilon = 1$ in the 1-loop result. Second column: Exponents obtained by setting $\epsilon = 1$ in the two-loop result. Third column: Conservative estimates based on three Padé estimates together with scaling relations between exponents.

$$= \frac{2\epsilon}{9} + \frac{\epsilon^2}{3}\left(\frac{10X^{(\alpha)}}{27} - \zeta_2\right) . \qquad \text{(IV.21)}$$

Specializing to the SR-case ($\alpha = 2$) yields with the help of (III.50)

$$\begin{aligned} z &= 2 - \Delta''(0^+) + \Delta''(0^+)^2 + \Delta'''(0^+)\Delta'(0^+)\left(\frac{3}{2} - \ln 2\right) \\ &= 2 - \frac{2\epsilon}{9} + \epsilon^2\left(\frac{\zeta_2}{3} - \frac{\ln 2}{54} - \frac{5}{108}\right) \\ &= 2 - 0.222222\epsilon - 0.0432087\epsilon^2 . \end{aligned} \qquad \text{(IV.22)}$$

The agreement with the numerical simulations given on figure IV.2 is again good. Finally, the exponents β and ν are obtained from scaling relations. For $\alpha = 2$ (SR) they read

$$\begin{aligned} \beta &= \frac{z-\zeta}{2-\zeta} \\ &= 1 - \frac{\epsilon}{9} + \epsilon^2\left(\frac{\zeta_2}{6} - \frac{1}{24} - \frac{\ln 2}{108}\right) \\ &= 1 - \frac{\epsilon}{9} + 0.040123\epsilon^2 \qquad \text{(IV.23)} \\ \nu &= \frac{1}{2-\zeta} = \frac{1}{2} + \frac{\epsilon}{12} + \epsilon^2\left(\frac{\zeta_2}{4} + \frac{1}{72}\right) \\ &= \frac{1}{2} + \frac{\epsilon}{12} + 0.0258316\,\epsilon^2 . \qquad \text{(IV.24)} \end{aligned}$$

We now turn to long range elasticity $\alpha \neq 2$. The general formula for z reads

$$z = \alpha - \frac{2}{9}\epsilon + \epsilon^2\left(\frac{\zeta_2}{3} - \frac{2X^{(\alpha)}}{27} + \frac{Y^{(\alpha)}}{54}\right) . \qquad \text{(IV.25)}$$

Specifying to $\alpha = 1$ yields

$$\begin{aligned} z &= 1 - \frac{2}{9}\epsilon + \epsilon^2\left(\frac{\zeta_2}{3} - \frac{\pi + 20\ln 2}{108}\right) \\ &= 1 - \frac{2}{9}\epsilon - 0.1132997\epsilon^2 . \end{aligned} \qquad \text{(IV.26)}$$

Again β and ν are obtained from scaling as ($\alpha = 1$)

$$\begin{aligned} \beta &= \frac{z-\zeta}{1-\zeta} = 1 - \frac{2}{9}\epsilon + \epsilon^2\left(\frac{\zeta_2}{3} - \frac{2}{27} - \frac{\pi + 20\ln 2}{108}\right) \\ &= 1 - \frac{2}{9}\epsilon - 0.1873737\epsilon^2 \qquad \text{(IV.27)} \\ \nu &= 1 + \frac{\epsilon}{3} + \epsilon^2\left(\frac{1}{9} + \zeta_2\right) \\ &= 1 + \frac{\epsilon}{3} + 0.24356\epsilon^2 . \qquad \text{(IV.28)} \end{aligned}$$

Numerical values are given on figure IV.3.

Note that to two loops at the RF fixed point there does not appear to be any unstable direction. We thus conclude, as in[21] that

$$\nu_{\rm FS} = \nu . \qquad \text{(IV.29)}$$

Finally, for depinning there should also be a family of fixed points corresponding to correlations of the *force* which are long range with $\Delta(u) \sim u^{-\alpha}$ and $\alpha \geq \alpha^* \geq 1$. The linear part of the FRG equation implies that $\zeta(\alpha) = \epsilon/(2+\alpha)$ and a crossover from the RF fixed point occurs when $\zeta(\alpha^*) = \zeta_{\rm RF} = \frac{\epsilon}{3} + \zeta_2\epsilon^2 + O(\epsilon^3)$. We have not studied these LR fixed points in details.

B. Periodic systems

exponent	dimension	1-loop	2-loop	estimate	simulation
	$d = 3$	0.83	0.78	0.78±0.03	0.81±0.03 0.84±0.05
β	$d = 2$	0.67	0.44	0.52±0.08	0.63±0.06 0.68±0.07
	$d = 1$	0.5	0.	0.2±0.2	

FIG. IV.4: Depinning exponents for CDW. First column: Exponents obtained by setting $\epsilon = 1$ in the 1-loop result. Second column: Exponents obtained by setting $\epsilon = 1$ in the two-loop result. Third column: Conservative estimates based on three Padé estimates, scaling relations and common sense. Fourth column: Simulations from[9].

For periodic $\Delta(u)$ as e.g. CDW depinning[17,21], there is another fixed point of (III.63). It is sufficient to study the case where the period is set to unity, all other cases are easily obtained using the reparametrization invariance of equation (IV.1). This means, that no rescaling is possible in that direction, and thus the rescaling factor is

$$\zeta = 0 . \qquad \text{(IV.30)}$$

The fixed-point function is then periodic, and can in the interval $[0,1]$ be expanded in a Taylor-series in $u(1-u)$. Evenmore, the ansatz

$$\Delta(u) = (a_1\epsilon + a_2\epsilon^2 + \ldots) + \left(b_1\epsilon + b_2\epsilon^2 + \ldots\right) u(1-u) \qquad \text{(IV.31)}$$

allows to satisfy the fixed-point equation (III.63) to order ϵ^2, with coefficients

$$\Delta^*(u) = \frac{\epsilon}{36} + \frac{\epsilon^2 X^{(\alpha)}}{108} - \left(\frac{\epsilon}{6} + \frac{\epsilon^2 X^{(\alpha)}}{9}\right) u(1-u) . \qquad \text{(IV.32)}$$

In the physically interesting situation of charge density waves, the elasticity is short range, i.e. $\alpha = 2$ and $X^{(\alpha)} = 1$ which yields:

$$\Delta^*(u) = \frac{\epsilon}{36} + \frac{\epsilon^2}{108} - \left(\frac{\epsilon}{6} + \frac{\epsilon^2}{9}\right) u(1-u) . \qquad \text{(IV.33)}$$

This fixed point is manifestly non-potential, i.e. it describes a force-force correlation-function, where the forces can not be derived from a potential. In a potential environment, the integral of the force over one period must vanish, and so must the force-force correlation-function. In contrast we find here

$$\int_0^1 {\rm d}u\, \Delta^*(u) = -\frac{\epsilon^2 X^{(\alpha)}}{108} \xrightarrow{\alpha\to 2} -\frac{\epsilon^2}{108} . \qquad \text{(IV.34)}$$

Thus to two loop the fixed point correctly accounts for the irreversibility in the driven system, which becomes manifest beyond the Larkin-length. This was not apparent to one loop.

An important feature of the periodic case is that the fixed point is *unstable*. The direction of instability is simply adding a constant to $\Delta(u)$ and its eigenvalue is trivial equal to ϵ to two loops and presumably to all orders. The full stability analysis is performed in appendix I but it can be seen already from:

$$-m\partial_m \int_0^1 \Delta(u)\,\mathrm{d}u = \epsilon \int_0^1 \Delta(u)\,\mathrm{d}u - 2X^{(\alpha)}\Delta'(0^+)^3 \tag{IV.35}$$

obtained by integration of the 2-loop FRG equation on the interval $[0^+, 1^-]$. One sees that $\int \Delta$ flows away if it does not coincide with its fixed point value (IV.34).

Thus the asymptotic flow as the dimensional parameter $m \to 0$ takes the simple form

$$\Delta_m(u) = \Delta^*(u) + cm^{-\epsilon} \tag{IV.36}$$

$$c = m_0^\epsilon \int_0^1 (\Delta_{m_0} - \Delta^*) \tag{IV.37}$$

i.e. it takes the fixed point form shifted by a growing constant. In the statics $\int_0^1 \mathrm{d}u\,\Delta_m = \int_0^1 \mathrm{d}u\,\Delta_* = 0$ from potentiality (the last term in (IV.35) is absent) and thus $c = 0$. At depinning c is non-zero at 2-loop order ($c \approx -\int_0^1 \Delta^* > 0$) using that the bare disorder has zero integral) and this has several consequences. First one obtains the static deformations as the sum

$$\overline{(u_x - u_0)^2} = B_{\mathrm{nl}}(x) + B_{\mathrm{RF}}(x) \tag{IV.38}$$

of a universal logarithmic growth-term

$$B_{\mathrm{nl}}(x) = A_d \ln|x| \tag{IV.39}$$

$$A_d = \frac{1}{18}\epsilon + \frac{2X^{(\alpha)} - 3}{108}\epsilon^2 \tag{IV.40}$$

(the calculation of A_d is presented in Appendix J as an example of an explicit calculation of a correlation function in the renormalized theory); and of the contribution of the generated "random force" of the Larkin type

$$B_{\mathrm{RF}}(x) \sim c|x|^{4-d}\,, \tag{IV.41}$$

which completely decouples from the other one. This is very similar to what was found in other driven systems where a random force is generated[50,66]. In particular this implies that the true roughness-exponent at depinning is not $\zeta = 0$ but

$$\zeta_{\mathrm{dep}} = \frac{4-d}{2}\,. \tag{IV.42}$$

Another consequence is that the the two exponents ν and ν_{FS} are different. We find:

$$\nu = \frac{1}{2-\zeta} = \frac{1}{2} \tag{IV.43}$$

$$\nu_{\mathrm{FS}} = \frac{1}{2-\zeta_{\mathrm{dep}}} = \frac{2}{d} \tag{IV.44}$$

and given the generality of the above argument this should holds to all orders. Note then that the CCFFS-bound[48] for ν_{FS} is saturated. This is very different to the case of interfaces (saturation of the bound there would lead to the incorrect result $\zeta = \epsilon/3$).

The dynamical exponent z is

$$z = \alpha - \frac{\epsilon}{3} - \frac{\epsilon^2 X^{(\alpha)}}{9} \xrightarrow{\alpha\to 2} 2 - \frac{\epsilon}{3} - \frac{\epsilon^2}{9}\,. \tag{IV.45}$$

Curiously, it does not depend on the diagram I_η or equivalently $Y^{(\alpha)}$.

In CDW depinning, the best observable quantity is β. From the scaling relation[17,19–21] $\beta = (z-\zeta)/(2-\zeta)$, and $\zeta = 0$, we find $\beta = z/2$ and thus for CDW ($\alpha = 2$)

$$\beta = 1 - \frac{\epsilon}{6} - \frac{\epsilon^2}{18}\,. \tag{IV.46}$$

This expansion is however ill-behaved, at least at large ϵ. It therefore seems advisable, to use one of the Pade-variants. The only one which respects common sense down to $d = 1$ and even beyond, is the Pade (0,2), reading

$$\beta = \frac{1}{1 + \frac{\epsilon}{6} + \frac{\epsilon^2}{12}}\,. \tag{IV.47}$$

Again simulations are in reasonable good agreement with our theoretical predictions, as can be seen on table IV.4. Further simulations would be welcome.

V. CONCLUSION

To conclude we have constructed a consistent field theory of isotropic depinning at zero temperature to 2-loop order. While the 1-loop flow-equations for statics and driven dynamics are identical, our 2-loop equations distinguish these physically different situations, yielding different universal predictions for both cases. This is an encouraging progress. The non-analytic field theory that we have developed here will be discussed in companion studies[34,35] for the static theory to two and three loops.

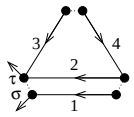
A lot remains to be done and understood. If universality is to hold at depinning then a renormalizable theory should exist to any number of loops. We have not attempted a proof to all orders here, and the mechanism in which the $1/\epsilon$-divergences cancel is non-trivial. We have however checked the applicability of formal constructions like the subtraction operator **R** on sample diagrams. This could further be tested in a 3-loop calculation. Although short time singularities ($\delta(vt)$ terms) did not appear their role to any order remains to be clarified. Next, effects of temperature have not been included here. One expects that although at $T = 0$ the statics and the depinning should be two distinct field theories, this distinction becomes blurred at finite temperature. How this will work out is not yet elucidated. Some efforts in that direction are reported in[77]. Similarly it would be quite interesting to understand how to describe $f = f_c^-$, i.e. the approach to the threshold from below. From the considerations here this appears to be quite non-trivial.

Extension of the present method to systems with $N > 1$ is also far from trivial. The monotonous increase of u_t does not apply to all components, which leads to complications. The large-N limit of the static FRG was solved exactly recently[36]and it would be interesting to extend it to the dynamics. Finally the threshold dynamics of other systems, such as random field spin models, which can be described by the FRG, is of interest.

From the point of view of simulations our results together with recent more powerful algorithms offer hope that more precise comparisons could be made, not only for exponents but also for other universal quantities which offer stronger tests such as scaling functions, amplitudes or finite size effects. The exponent $\nu_{\rm FS}$ should be measured independently. We encourage further precise numerical studies on both manifolds and CDW with a comparison to theory in mind. Agreement between numerics and theory would allow to rule out or to accept elastic models for the description of more complex experimental situations.

APPENDIX A: CORRECTIONS TO DISORDER: DIAGRAMS OF TYPE A

In the following, we give explicit expressions for the diagrams contributing to the renormalization of disorder. To simplify notations, we have introduced $q_3 := q_1 - q_2$ and set the mass m to zero. The mass-dependence can easily be reconstructed by replacing q_i^2 by $q_i^2 + m^2$. We start with the diagrams of class A, given on figure III.4. For illustration, we show the complete calculation of the first non-vanishing diagram a_2:



$$= -\int_{q_1,q_2}\int_{t_1,t_2,t_3,t_4>0} \mathrm{e}^{-q_1^2 t_1 - q_2^2 t_2 - q_3^2(t_3+t_4)} \times\Delta'''(u_\tau - u_\sigma)\Delta'(u_{\tau-t_2} - u_{\sigma-t_1}) \times\Delta(u_{\tau-t_3} - u_{\tau-t_2-t_4})\,. \qquad \text{(A.1)}$$

For the field u, we have given the time-arguments, but suppressed the spatial arguments, since the result is taken at constant background field. We also do not write explicitly the two response-fields. The given configuration is for $\tau - \sigma$ large, and we can set $u := u_{\tau'} - u_{\sigma'}$ for all $\tau' = \tau \pm$ some t_i, $\sigma' = \sigma \pm$ some t_i since the t_i are small (due to the exponentially suppressing factors) compared to the difference of $\tau - \sigma$. Finally, since Δ is continuous, $\Delta(u_{\tau-t_3} - u_{\tau-t_2-t_4})$ can be replaced by $\Delta(0)$. Integrating over all times leads to

$$\mathrm{a}_2 = -2\Delta(0)\Delta'(u)\Delta'''(u)\int_{q_1,q_2}\frac{1}{q_1^2 q_2^2 q_3^4}\,. \qquad \text{(A.2)}$$

Similarly, we find

$$\mathrm{a}_3 = -2\Delta(0)\Delta''(u)^2\int_{q_1,q_2}\frac{1}{q_1^2 q_2^2 q_3^4} \qquad \text{(A.3)}$$

$$\mathrm{a}_2 + \mathrm{a}_3 = -\partial_u^2\left[\Delta(0)\Delta'(u)^2\int_{q_1,q_2}\frac{1}{q_1^2 q_2^2 q_3^4}\right] \qquad \text{(A.4)}$$

$$\mathrm{b}_1 = 2\Delta'(u)^2\Delta''(u)\int_{q_1,q_2}\frac{1}{q_1^2 q_2^2 q_3^4} \qquad \text{(A.5)}$$

$$\mathrm{b}_2 = 2\Delta(u)\Delta'(u)\Delta'''(u)\int_{q_1,q_2}\frac{1}{q_1^2 q_2^2 q_3^4} \qquad \text{(A.6)}$$

$$\mathrm{b}_3 = \Delta(u)\Delta''(u)^2\int_{q_1,q_2}\frac{1}{q_1^2 q_2^2 q_3^4} \qquad \text{(A.7)}$$

$$\mathrm{b}_4 = \Delta''(u)\Delta'(u)^2\int_{q_1,q_2}\frac{1}{q_1^2 q_2^2 q_3^4} \qquad \text{(A.8)}$$

$$\mathrm{b}_5 = 2\Delta''(u)\Delta'(u)^2\int_{q_1,q_2}\frac{1}{q_1^2 q_2^2 q_3^4} \qquad \text{(A.9)}$$

$$\mathrm{b}_6 = \Delta(u)\Delta''(u)^2\int_{q_1,q_2}\frac{1}{q_1^2 q_2^2 q_3^4}\,. \qquad \text{(A.10)}$$

The contribution of the b_i's can be summed as

$$\sum_{i=1}^{6}\mathrm{b}_i = \partial_u^2\left[\Delta(u)\Delta'(u)^2\int_{q_1,q_2}\frac{1}{q_1^2 q_2^2 q_3^4}\right]\,. \qquad \text{(A.11)}$$

Diagram c_1 is

$$\mathrm{c}_1 = 2\Delta'(0^+)^2\Delta''(u)\int_{q_1,q_2}\frac{1}{q_1^2 q_2^2 q_3^4}\,. \qquad \text{(A.12)}$$

All these diagrams contain the hat-diagram known from the statics and ϕ^4 theory. It can be calculated as follows:



$$\begin{aligned}
&= \int_{q_1,q_2}\frac{1}{(q_1^2+m^2)(q_2^2+m^2)^2((q_1+q_2)^2+m^2)} = \int_{\alpha,\beta,\gamma>0}\beta\mathrm{e}^{-\alpha(q_1^2+m^2)-\beta(q_2^2+m^2)-\gamma((q_1+q_2)^2+m^2)}\\
&= \left(\int_q \mathrm{e}^{-q^2}\right)^2\int_{\alpha>0,\beta>0,\gamma>0}\beta\mathrm{e}^{-m^2(\alpha+\beta+\gamma)}\left[\mathrm{Det}\begin{pmatrix}\alpha+\gamma & \gamma\\ \gamma & \beta+\gamma\end{pmatrix}\right]^{-d/2}\\
&= \left(\int_q \mathrm{e}^{-q^2}\right)^2\int_{\alpha>0,\beta>0,\gamma>0}\beta\gamma^{3-d}\mathrm{e}^{-m^2\gamma(\alpha+\beta+1)}(\alpha+\beta+\alpha\beta)^{-d/2}\\
&= \left(\int_q \mathrm{e}^{-q^2}\right)^2\Gamma(4-d)m^{-2\epsilon}J\,, \qquad \text{(A.13)}
\end{aligned}$$

where we split the divergent integral J in pieces, which are either finite or where the divergence can be calculated analytically:

$$J = \int_0^\infty \mathrm{d}\alpha \int_0^\infty \mathrm{d}\beta \, \frac{\beta}{(\alpha+\beta+\alpha\beta)^2} \frac{(\alpha+\beta+\alpha\beta)^{\frac{\epsilon}{2}}}{(\alpha+\beta+1)^\epsilon} = J_1 + J_2 + J_3 \tag{A.14}$$

$$J_1 = \int_0^\infty \mathrm{d}\alpha \int_0^1 \mathrm{d}\beta \, \frac{\beta}{(\alpha+\beta+\alpha\beta)^2} \frac{(\alpha+\beta+\alpha\beta)^{\frac{\epsilon}{2}}}{(\alpha+\beta+1)^\epsilon} = \ln 2 + O(\epsilon) \tag{A.15}$$

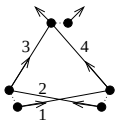
$$J_2 = \int_0^\infty \mathrm{d}\alpha \int_1^\infty \mathrm{d}\beta \left(\frac{\beta}{(\alpha+\beta+\alpha\beta)^2} \frac{(\alpha+\beta+\alpha\beta)^{\frac{\epsilon}{2}}}{(\alpha+\beta+1)^\epsilon} - \frac{1}{(1+\alpha)^{2-\frac{\epsilon}{2}}\beta^{1+\frac{\epsilon}{2}}} \right) = -\ln 2 + O(\epsilon) \tag{A.16}$$

$$J_3 = \int_0^\infty \mathrm{d}\alpha \int_1^\infty \mathrm{d}\beta \, \frac{1}{(1+\alpha)^{2-\frac{\epsilon}{2}}\beta^{1+\frac{\epsilon}{2}}} = \frac{2}{\epsilon} + 1 + O(\epsilon) \tag{A.17}$$

This gives the final result for the hat-diagram

$$I_A = \quad = \left(\int_q \mathrm{e}^{-q^2} \right)^2 \Gamma(4-d)\, m^{-2\epsilon} \left(\frac{2}{\epsilon} + 1 + O(\epsilon) \right)$$
$$= \left(\frac{1}{2\epsilon^2} + \frac{1}{4\epsilon} \right) \left(\epsilon I_1^{(\alpha)} \right)^2 . \tag{A.18}$$

We now turn to the non-trivial diagram e_1. At finite velocity v, the diagram is



$$= \int_{q_1,q_2} \int_{t_1,\ldots,t_4>0} \Delta''(u)\Delta'(v(t_1+t_4-t_3)) \times \Delta'(v(t_2+t_3-t_4))\mathrm{e}^{-t_1 q_1^2 - t_2 q_2^2 - (t_3+t_4)q_3^3} \tag{A.19}$$

In the limit of vanishing velocity $v \to 0$, we can replace $\Delta'(v(t_2+t_3-t_4))$ by $\Delta(0^+)\mathrm{sgn}(t_2+t_3-t_4)$ a.s.o. Let us stress that this replacement is correct both before and after reaching the Larkin length. Its result is

$$\mathrm{e}_1 = \Delta'(0^+)^2\Delta''(u) \times \int_{q_1,q_2} \int_{t_3,t_4>0} \mathrm{e}^{-q_3^2(t_3+t_4)} I(t_3,t_4,q_1,q_2) \tag{A.20}$$

$$I(t_3,t_4,q_1,q_2) = \int_{t_1,t_2} \theta(t_1)\theta(t_2)\mathrm{sgn}(t_1+t_4-t_3) \times \mathrm{sgn}(t_2+t_3-t_4)\mathrm{e}^{-(q_1^2 t_1 + q_2^2 t_2)} . \tag{A.21}$$

Using that $\mathrm{e}^{-(q_1^2 t_1 + q_2^2 t_2)} = \frac{1}{q_1^2 q_2^2}\partial_{t_1}\partial_{t_2}\mathrm{e}^{-(q_1^2 t_1 + q_2^2 t_2)}$ and integrating I by parts in t_1 and t_2 yields

$$I(t_3,t_4,q_1,q_2) = \frac{1}{q_1^2 q_2^2} \times \Big[2\theta(t_3-t_4)\mathrm{e}^{-q_1^2(t_3-t_4)} + 2\theta(t_4-t_3)\mathrm{e}^{-q_2^2(t_4-t_3)} - 1) \Big] \tag{A.22}$$

The integral over the two remaining times t_3 and t_4 in (A.20) gives

$$\int_{t_3,t_4>0} I(t_3,t_4,q_1,q_2) = \frac{1}{q_1^2 q_2^2} \left(\frac{1}{q_3^2(q_1^2+q_3^2)} + \frac{1}{q_3^2(q_2^2+q_3^2)} - \frac{1}{q_3^4} \right) \tag{A.23}$$

and thus

$$\mathrm{e}_1 = \Delta'(0^+)^2\Delta''(u) \times \times \int_{q_1,q_2} \frac{1}{q_1^2 q_2^2 q_3^2} \left(\frac{1}{q_1^2+q_3^2} + \frac{1}{q_2^2+q_3^2} - \frac{1}{q_3^2} \right) \tag{A.24}$$

with $q_3 = q_1 - q_2$. In presence of a mass this reads:

$$\mathrm{e}_1 = \Delta'(0^+)^2\Delta''(u) \times \times \int_{q_1,q_2} \frac{1}{(q_1^2+m^2)(q_2^2+m^2)(q_3^2+m^2)} \left(\frac{1}{q_1^2+q_3^2+2m^2} + \frac{1}{q_2^2+q_3^2+2m^2} - \frac{1}{q_3^2+m^2} \right) \tag{A.25}$$

We now calculate the new integral. It is relatively simple, since it has only a single pole in $1/\epsilon$:

$$I_l := \int_{q_1,q_2} \frac{1}{(q_1^2+m^2)(q_2^2+m^2)(q_3^2+m^2)(q_1^2+q_3^2+2m^2)} = \int_{q_1,q_3} \int_{\alpha>0,\beta>0,\gamma>0,\delta>0} \mathrm{e}^{-\alpha(q_1^2+m^2)-\beta((q_1+q_3)^2+m^2)-\gamma(q_3^2+m^2)-\delta(q_1^2+q_3^2+2m^2)}$$

$$
\begin{aligned}
&= \left(\int_q \mathrm{e}^{-q^2}\right)^2 \int_{\alpha>0,\beta>0,\gamma>0,\delta>0} \mathrm{e}^{-m^2(\alpha+\beta+\gamma+2\delta)} \left[\mathrm{Det}\begin{pmatrix} \alpha+\beta+\delta & \beta \\ \beta & \beta+\delta+\gamma \end{pmatrix}\right]^{-d/2} \\
&= \left(\int_q \mathrm{e}^{-q^2}\right)^2 \int_{\alpha>0,\beta>0,\gamma>0,\delta>0} \mathrm{e}^{-m^2\delta(\alpha+\beta+\gamma+2)} \delta^{3-d} (1+\gamma+\alpha+2\beta+\alpha\beta+\alpha\gamma+\beta\gamma)^{-d/2} \\
&= \Gamma(4-d) \left(\int_q \mathrm{e}^{-q^2}\right)^2 \int_{\alpha>0,\beta>0,\gamma>0} (1+\gamma+\alpha+2\beta+\alpha\beta+\alpha\gamma+\beta\gamma)^{-d/2} \left[m^2(\alpha+\beta+\gamma+2)\right]^{d-4} \\
&= \left(\int_q \mathrm{e}^{-q^2}\right)^2 \frac{1}{\epsilon} m^{-2\epsilon} \int_{\alpha>0,\beta>0,\gamma>0} (1+\gamma+\alpha+2\beta+\alpha\beta+\alpha\gamma+\beta\gamma)^{-2} + \text{finite} \\
&= 2\ln 2 \left(\int_q \mathrm{e}^{-q^2}\right)^2 \frac{1}{\epsilon} m^{-2\epsilon} + \text{ finite} \\
&= \frac{\ln 2}{2\epsilon} (\epsilon I_1)^2 + \text{finite}
\end{aligned} \tag{A.26}
$$

This gives the final result for e_1

$$\mathrm{e}_1 = \Delta'(0^+)^2 \Delta''(u) \left(2I_l - I_A\right) . \tag{A.27}$$

The last non-vanishing diagram is f_2:

$$\mathrm{f}_2 = 2\Delta'(0^+)^2\Delta''(u) \int_{q_1,q_2} \mathrm{e}^{-q_3^2(t_3+t_4)-(q_1^2 t_1+q_2^2 t_2)} \times \\ \times \mathrm{sgn}(t_4-t_3-t_2) . \tag{A.28}$$

Integrating first over t_4 and then over the remaining times gives

$$\mathrm{f}_2 = -2\Delta'(0^+)^2\Delta''(u) \int_{q_1,q_2} \frac{1}{q_1^2 q_2^2 q_3^2 (q_2^2+q_3^2)} . \tag{A.29}$$

The integral has already been calculated in (A.26), yielding the result

$$\mathrm{f}_2 = -2\Delta'(0^+)^2\Delta''(u) I_l . \tag{A.30}$$

Note that the non-trivial integrals in e_1 and f_2 are in fact identical and cancel:

$$\mathrm{e}_1 + \mathrm{f}_2 = -\Delta'(0^+)^2\Delta''(u) I_A . \tag{A.31}$$

APPENDIX B: CORRECTIONS TO DISORDER: DIAGRAMS OF TYPE B

In this appendix, we calculate diagrams of type B (the bubble-chains).

The diagrams which are odd functions of u are:

$$\mathrm{h}_1 = \mathrm{h}_2 = \mathrm{i}_1 = \mathrm{j}_1 = \mathrm{k}_2 = \mathrm{k}_3 = \mathrm{l}_2 = \mathrm{l}_3 = \mathrm{l}_4 = 0 . \tag{B.1}$$

The diagrams that are second derivative of static ones have all their response-fields on their unsaturated vertices. These are:

$$\mathrm{g}_1 = \Delta''(u)^2 \Delta I_1^2 \tag{B.2}$$
$$\mathrm{g}_2 = 2\Delta'(u)\Delta'''(u)\Delta(u) I_1^2 \tag{B.3}$$
$$\mathrm{g}_3 = \Delta'(u)^2\Delta''(u) I_1^2 \tag{B.4}$$
$$\mathrm{g}_4 = \frac{1}{2}\Delta(u)^2\Delta''''(u) I_1^2 \tag{B.5}$$
$$\mathrm{g}_1+\mathrm{g}_2+\mathrm{g}_3+\mathrm{g}_4 = \partial_u^2 \left[\frac{1}{2}\Delta(u)^2\Delta''(u)\right] I_1^2 \tag{B.6}$$
$$\mathrm{h}_3 = -\Delta(0)\Delta''''(u)\Delta(u) I_1^2 \tag{B.7}$$
$$\mathrm{h}_4 = -\Delta(0)\Delta''(u)^2 I_1^2 \tag{B.8}$$
$$\mathrm{h}_5 = \mathrm{h}_6 = -\Delta(0)\Delta'''(u)\Delta'(u) I_1^2 \tag{B.9}$$
$$\mathrm{h}_3+\mathrm{h}_4+\mathrm{h}_5+\mathrm{h}_6 = \partial_u^2 \left[-\Delta(0)\Delta(u)\Delta''(u)\right] I_1^2 \tag{B.10}$$
$$\mathrm{i}_2 = \mathrm{j}_2 = \frac{1}{4}\Delta(0)^2\Delta''''(u) I_1^2 \tag{B.11}$$
$$\mathrm{k}_1 = -\mathrm{l}_1 = -\Delta(u)''\Delta''(0^+)\Delta(0) I_1^2 . \tag{B.12}$$

The surprise is that i_3, which is not the second derivative of a static diagram (since it has both $\hat{u}$ on saturated vertices) is non-trivial:

$$\mathrm{i}_3 = -\Delta'(0^+)^2\Delta''(u) I_1^2 . \tag{B.13}$$

This diagram is necessary to ensure renormalizability.

APPENDIX C: CORRECTIONS TO DISORDER: DIAGRAMS OF TYPE C

In this appendix, we show that diagrams of type C do not contribute to the renormalization of disorder. This is fortunate, since they involve a strongly diverging diagram (the tadpole), which would render perturbation theory non-universal.

The diagrams which are odd functions of u are

$$\mathrm{m}_1 = \mathrm{m}_3 = \mathrm{m}_4 = \mathrm{m}_5 = \mathrm{n}_1 = \mathrm{n}_3 \\ = \mathrm{n}_4 = \mathrm{n}_5 = \mathrm{p}_2 = \mathrm{p}_3 = \mathrm{q}_2 = \mathrm{q}_3 = 0 . \tag{C.1}$$

The following diagrams cancel:

$$\mathrm{m}_2 + \mathrm{n}_2 = 0 \tag{C.2}$$
$$\mathrm{p}_1 + \mathrm{q}_1 = 0 \tag{C.3}$$
$$\mathrm{p}_4 + q_4 = 0 . \tag{C.4}$$

No contribution remains.

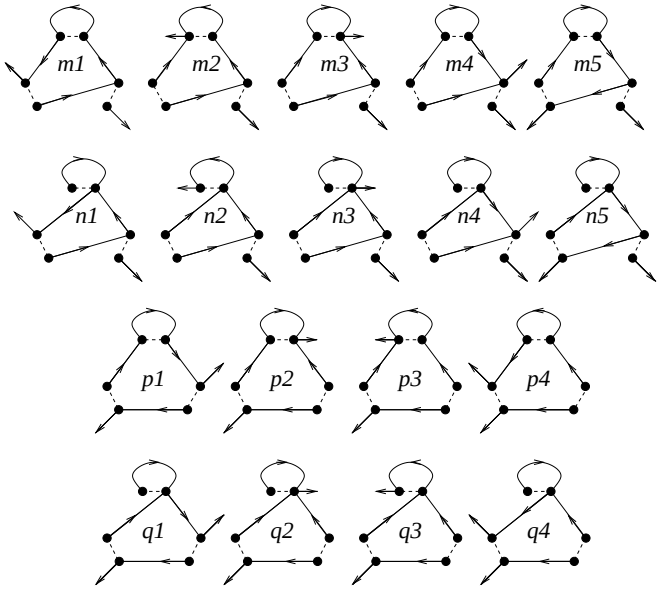
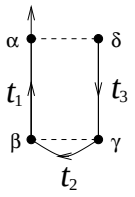


FIG. C.1: 2-loop diagrams of class C

APPENDIX D: CORRECTIONS TO η: 2-LOOP DIAGRAMS

In this appendix, we give all diagrams contributing to the correction of η at second order. For simplicity of notation, we again drop the explicit mass-dependence. We group together those diagrams which partially cancel. We demonstrate explicitly how to calculate the first diagram a from the very beginning.

$$\mathrm{a} = \quad \text{(D.1)}$$



$$= \int_{q_1,q_2} \int_{t_1,t_2,t_3} R_{q_1 t_1} R_{q_2 t_2} R_{q_1 t_3} \times \Delta'(u_{t=0} - u_{-t_1-t_2-t_3})(-\Delta''(u_{-t_1}))$$

We have drawn three response functions. We have chosen to start counting time at 0 for vertex α, such that vertex β is at time $-t_1$, vertex γ at time $-t_1 - t_2$ and vertex δ at time $-t_1-t_2-t_3$. This gives the times for the arguments of Δ. The upper Δ in diagram a has one time derivative, the lower vertex two, resulting in Δ' and $-\Delta''$ respectively (the minus-sign is a consequence of the both response-functions entering at different "ends" of Δ). We have suppressed the space-arguments in the fields u, since all diagrams correcting η are calculated at a spatially constant background field. Inserting the response-functions $R_{qt} = \Theta(t)\mathrm{e}^{-q^2 t}$, we arrive at

$$\mathrm{a} = -\int_{q_1,q_2} \int_{t_1,t_2,t_3>0} \mathrm{e}^{-q_1^2(t_1+t_3)-q_2^2 t_2} \times \Delta'(u_0 - u_{-t_1-t_2-t_3})\Delta''(u_{-t_1} - u_{-t_1-t_2}) \quad \text{(D.2)}$$

The crucial point is now that this diagram corrects the critical force and η. The correction to the critical force is obtained by setting the arguments of the Δ's to 0^+ (unique here due to the time-arguments). This contribution is non-universal and we shall not calculate it in the following. The *universal* correction to η is obtained by Taylor-expanding the argument of e.g. $\Delta'(u_0 - u_{-t_1-t_2-t_3})$ as

$$u_0 - u_{-t_1-t_2-t_3} \approx (v + \dot{u}_0)(t_1 + t_2 + t_3) \quad \text{(D.3)}$$

and thus

$$\Delta'(u_0 - u_{-t_1-t_2-t_3}) \approx \Delta''(0^+)\dot{u}_0(t_1 + t_2 + t_3)\,, \quad \text{(D.4)}$$

which naturally leads to the generation of a correction to friction. For our diagram, this is (sloppily dropping $\dot{u}_0$ and the response-field for simplicity of notation)

$$\begin{aligned}\mathrm{a} &= -\int_{q_1,q_2} \int_{t_1,t_2,t_3>>0} \mathrm{e}^{-q_1^2(t_1+t_3)-q_2^2 t_2} \times \left[\Delta''(0^+)^2(t_1+t_2+t_3) + \Delta'(0^+)\Delta'''(0^+)t_2\right] \\ &= -\int_{q_1,q_2} \Delta''(0^+)^2 \left(\frac{2}{q_1^6 q_2^2} + \frac{1}{q_1^4 q_2^4}\right) + \Delta'(0^+)\Delta'''(0^+)\frac{1}{q_1^4 q_2^4}\end{aligned} \quad \text{(D.5)}$$

where in the last line we have explicitly performed the time-integrations.

Diagram g is

$$\begin{aligned}\mathrm{g} &= \int_{q_1,q_2} \int_{t_1,t_2,t_3>0} \mathrm{e}^{-q_1^2(t_1+t_3)-q_2^2 t_2} \times \Delta'(u_0 - u_{-t_1-t_3})\Delta''(u_{-t_1} - u_{-t_1-t_2}) \\ &= \int_{q_1,q_2} \int_{t_1,t_2,t_3>0} \mathrm{e}^{-q_1^2(t_1+t_3)-q_2^2 t_2} \times \left(\Delta''(0^+)^2(t_1+t_3) + \Delta'(0^+)\Delta'''(0^+)t_2\right) \\ &= \int_{q_1,q_2} \Delta''(0^+)^2 \frac{2}{q_1^6 q_2^2} + \Delta'(0^+)\Delta'''(0^+)\frac{1}{q_1^4 q_2^4}\,.\end{aligned} \quad \text{(D.6)}$$

Thus

$$\mathrm{a} + \mathrm{g} = -\int_{q_1,q_2} \Delta''(0^+)^2 \frac{1}{q_1^4 q_2^4} = -\Delta''(0^+)^2 I_1^2 \quad \text{(D.7)}$$

Note that both diagrams a and g contain a tadpole-like subdivergence, which is canceled by a counter-term for the critical force. However their sum does not involve such a term and thus there is no need to specify it.

Graphs b, c and d:

$$\mathrm{b} = -\int_{q_1,q_2} \int_{t_1,t_2,t_3>0} \mathrm{e}^{-q_1^2(t_1+t_3)-q_2^2 t_2} \times$$

$$\Delta'''(u_0-u_{-t_2})\Delta(u_{-t_3}-u_{-t_1-t_2})$$
$$= -\int_{q_1,q_2}\int_{t_1,t_2,t_3} \mathrm{e}^{-q_1^2(t_1+t_3)-q_2^2t_2}\times \left[\Delta''''(0^+)\Delta(0)t_2+\Delta'''(0^+)\Delta'(0^+)|t_1+t_2-t_3|\right] \tag{D.8}$$

while

$$\mathrm{c}=\mathrm{d}=\frac{1}{2}\int_{q_1,q_2}\int_{t_1,t_2,t_3>0} \mathrm{e}^{-q_1^2(t_1+t_3)-q_2^2t_2}\times \left[\Delta''''(0^+)\Delta(0)t_2+\Delta'''(0^+)\Delta'(0^+)|t_1-t_3|\right]. \tag{D.9}$$

Note the factor $1/2$ for the symmetry in the lower vertex. Together they are

$$\mathrm{b}+\mathrm{c}+\mathrm{d}=\Delta'''(0^+)\Delta'(0^+) \times\int_{q_1,q_2}\int_{t_1,t_2,t_3} \mathrm{e}^{-q_1^2(t_1+t_3)-q_2^2t_2}(|t_1-t_3|-|t_1+t_2-t_3|) \tag{D.10}$$

Changing variables to $u=t_1-t_3$ and $s=\frac{1}{2}(t_1+t_3)$, the integral $\int_{t_1,t_3>0}$ becomes $\int_0^\infty \mathrm{d}s\int_{-2s}^{2s}\mathrm{d}u$. The integral over u can be performed, but for fixed s the second term in (D.10) depends on the value of t_2. Distinguishing the both cases, we obtain

$$\begin{aligned}\mathrm{b}+\mathrm{c}+\mathrm{d}&=\Delta'''(0^+)\Delta'(0^+)\int_{q_1,q_2}\int_{s>0}\mathrm{e}^{-2q_1^2s}\left[\int_0^\infty \mathrm{d}t_2\,\mathrm{e}^{-q_2^2t_2}4s^2-\int_0^{2s}\mathrm{d}t_2\,\mathrm{e}^{-q_2^2t_2}(t_2^2+4s^2)-\int_{2s}^\infty \mathrm{d}t_2\,\mathrm{e}^{-q_2^2t_2}4st_2\right]\\ &=-\Delta'''(0^+)\Delta'(0^+)\int_{q_1,q_2}\frac{1}{q_1^2q_2^4(q_1^2+q_2^2)}\,.\end{aligned} \tag{D.11}$$

This integral can be simplified through symmetrization. Using that

$$\int_{q_1,q_2}\left[\frac{1}{q_1^2q_2^4(q_1^2+q_2^2)}+\frac{1}{q_1^4q_2^2(q_1^2+q_2^2)}\right]=\int_{q_1,q_2}\frac{1}{q_1^4q_2^4}=I_1^2\,, \tag{D.12}$$

we obtain

$$\mathrm{b}+\mathrm{c}+\mathrm{d}=-\frac{1}{2}\Delta'''(0^+)\Delta'(0^+)I_1^2\,. \tag{D.13}$$

The next diagram is e:

$$\begin{aligned}\mathrm{e}&=\int_{q_1,q_2}\int_{t_1,t_2,t_3}\mathrm{e}^{-q_1^2t_1-q_2^2t_2-q_3^2t_3}\Delta''(u_0-u_{-t_2-t_1}))\Delta'(u_{-t_2}-u_{-t_3})\\ &=\int_{q_1,q_2}\int_{t_1,t_2,t_3}\mathrm{e}^{-q_1^2t_1-q_2^2t_2-q_3^2t_3}\left[\Delta'''(0^+)\Delta'(0^+)(t_2+t_1)\,\mathrm{sgn}(t_3-t_2)+\Delta''(0^+)^2(t_3-t_2)\right]\,.\end{aligned} \tag{D.14}$$

By symmetrizing in $(2\leftrightarrow 3)$, the term proportional to t_1 and the term proportional to (t_3-t_2) vanish. The remaining term can be written as

$$\mathrm{e}=-\frac{1}{2}\int_{q_1,q_2}\int_{t_1,t_2,t_3}\mathrm{e}^{-q_1^2t_1-q_2^2t_2-q_3^2t_3}\Delta'''(0^+)\Delta'(0^+)|t_2-t_3|\,. \tag{D.15}$$

Making the same change of variables to u and s as for (D.11), the integration over u, s and t_1 can be performed in this order, distinguishing the cases $u<0$ and $u>0$. Both cases give the same result for a total of

$$\mathrm{e}=-\Delta'''(0^+)\Delta'(0^+)\int_{q_1,q_2}\frac{1}{q_1^2q_2^4(q_2^2+q_3^2)}\,. \tag{D.16}$$

This contains the new integral (given regularized)

$$I_\eta:=\int_{q_1,q_2}\frac{1}{(q_1^2+m^2)(q_2^2+m^2)^2(q_2^2+q_3^2+2m^2)}\,. \tag{D.17}$$

It is related to I_l, see (A.26) and I_A, see (A.18):

$$I_\eta + I_l = I_A \ . \tag{D.18}$$

It is calculated in appendix E. The last diagram to be calculated is f:

$$\begin{aligned}
\mathrm{f} &= \int_{q_1,q_2}\int_{t_1,t_2,t_3} \mathrm{e}^{-q_1^2 t_1 - q_2^2 t_2 - q_3^2 t_3}\,\Delta''(u_0 - u_{-t_1-t_2})\Delta'(u_{-t_1-t_2-t_3} - u_{-t_2}) \\
&= -\int_{q_1,q_2}\int_{t_1,t_2,t_3} \mathrm{e}^{-q_1^2 t_1 - q_2^2 t_2 - q_3^2 t_3}\left[\Delta'''(0^+)\Delta'(0^+)(t_2+t_1) + \Delta''(0^+)^2(t_1+t_3)\right] \\
&= -2\Delta'''(0^+)\Delta'(0^+)I_A - 2\Delta''(0^+)^2 I_A \ .
\end{aligned} \tag{D.19}$$

APPENDIX E: THE INTEGRAL I_η

We have to calculate the integral I_η defined as

$$I_\eta := \int_{q_1,q_2} \frac{1}{(q_1^2+m^2)(q_2^2+m^2)^2(q_2^2+q_3^2+2m^2)} \ . \tag{E.1}$$

This is done as follows:

$$\begin{aligned}
I_\eta &= \int_{q_1,q_2}\int_{\alpha,\beta,\gamma>0} \beta\,\mathrm{e}^{-\alpha(q_1^2+m^2)-\beta(q_2^2+m^2)-\gamma(q_2^2+q_3^2+2m^2)} \\
&= \left(\int_q \mathrm{e}^{-q^2}\right)^2 \int_{\alpha,\beta,\gamma>0} \beta\,\mathrm{e}^{-m^2(\alpha+\beta+2\gamma)} \left[\mathrm{Det}\begin{pmatrix}\alpha+\gamma & \gamma \\ \gamma & \beta+2\gamma\end{pmatrix}\right]^{-d/2} \\
&= \left(\int_q \mathrm{e}^{-q^2}\right)^2 \int_{\alpha,\beta,\gamma>0} \beta\,\gamma^{3-d}\mathrm{e}^{-m^2\gamma(\alpha+\beta+2)}(1+2\alpha+\beta+\alpha\beta)^{-d/2} \\
&= \left(\int_q \mathrm{e}^{-q^2}\right)^2 \Gamma(4-d)\,m^{-2\epsilon}\,J
\end{aligned} \tag{E.2}$$

with

$$J := \int_0^\infty \mathrm{d}\alpha \int_0^\infty \mathrm{d}\beta\, \frac{\beta}{(1+2\alpha+\beta+\alpha\beta)^2} \frac{(1+2\alpha+\beta+\alpha\beta)^{\frac{\epsilon}{2}}}{(\alpha+\beta+2)^\epsilon} = J_1 + J_2 + J_3 \tag{E.3}$$

$$J_1 := \int_0^\infty \mathrm{d}\alpha \int_0^1 \mathrm{d}\beta\, \frac{\beta}{(1+2\alpha+\beta+\alpha\beta)^2} \frac{(1+2\alpha+\beta+\alpha\beta)^{\frac{\epsilon}{2}}}{(\alpha+\beta+2)^\epsilon} = 2\ln 3 - 3\ln 2 + O(\epsilon) \tag{E.4}$$

$$J_2 := \int_0^\infty \mathrm{d}\alpha \int_1^\infty \mathrm{d}\beta\, \left[\frac{\beta}{(1+2\alpha+\beta+\alpha\beta)^2} \frac{(1+2\alpha+\beta+\alpha\beta)^{\frac{\epsilon}{2}}}{(\alpha+\beta+2)^\epsilon} - \frac{1}{(1+\alpha)^{2-\frac{\epsilon}{2}}\beta^{1+\frac{\epsilon}{2}}}\right] = \ln 2 - 2\ln 3 + O(\epsilon) \tag{E.5}$$

$$J_3 := \int_0^\infty \mathrm{d}\alpha \int_1^\infty \mathrm{d}\beta\, \frac{1}{(1+\alpha)^{2-\frac{\epsilon}{2}}\beta^{1+\frac{\epsilon}{2}}} = \frac{2}{\epsilon} + 1 + O(\epsilon) \ . \tag{E.6}$$

Thus

$$I_\eta := \int_{q_1,q_2} \frac{1}{(q_1^2+m^2)(q_2^2+m^2)^2(q_2^2+q_3^2+2m^2)} = \left(\frac{1}{2\epsilon^2} + \frac{1-2\ln 2}{4\epsilon}\right)(\epsilon I_1)^2 + \text{finite} \ . \tag{E.7}$$

APPENDIX F: INTEGRALS IN LONG RANGE ELASTICITY CALCULATION

In the long-range case, there are two integrals which contribute to the renormalization of the disorder. At 1-loop order this is

$$\begin{aligned}
I_1^{(\alpha)} &:= \int_q \frac{1}{(q^2+m^2)^\alpha} = \frac{1}{\Gamma(\alpha)}\int_0^\infty \frac{\mathrm{d}s}{s} s^\alpha \int_q \mathrm{e}^{-s(q^2+m^2)} \\
&= m^{-\epsilon}\frac{\Gamma(\frac{\epsilon}{2})}{\Gamma(\alpha)}\left(\int_q \mathrm{e}^{-q^2}\right) \ .
\end{aligned} \tag{F.1}$$

At 2-loop order, this is

$$I_A^{(\alpha)} := \int\limits_{q_1,q_2} \frac{1}{(q_1^2+m^2)^{\frac{\alpha}{2}}(q_2^2+m^2)^{\alpha}((q_1+q_2)^2+m^2)^{\frac{\alpha}{2}}} \tag{F.2}$$

This is evaluated as follows

$$\begin{aligned} I_A^{(\alpha)} &= \int_0^\infty \frac{\mathrm{d}s}{s}\frac{s^{\frac{\alpha}{2}}}{\Gamma(\frac{\alpha}{2})}\int_0^\infty \frac{\mathrm{d}t}{t}\frac{t^{\alpha}}{\Gamma(\alpha)}\int_0^\infty \frac{\mathrm{d}u}{u}\frac{u^{\frac{\alpha}{2}}}{\Gamma(\frac{\alpha}{2})} \\ &\quad\times \int_{q_1,q_2} \mathrm{e}^{-s(q_1^2+m^2)-t(q_2^2+m^2)-u((q_1+q_2)^2+m^2)} \\ &= \left(\int_q \mathrm{e}^{-q^2}\right)^2 \int_0^\infty \frac{\mathrm{d}s}{s}\frac{s^{\frac{\alpha}{2}}}{\Gamma(\frac{\alpha}{2})}\int_0^\infty \frac{\mathrm{d}t}{t}\frac{t^{\alpha}}{\Gamma(\alpha)}\int_0^\infty \frac{\mathrm{d}u}{u}\frac{u^{\frac{\alpha}{2}}}{\Gamma(\frac{\alpha}{2})} \\ &\quad\times \left[\det\begin{pmatrix} s+u & u \\ u & t+u\end{pmatrix}\right]^{-\frac{d}{2}} \mathrm{e}^{-(s+t+u)m^2} \end{aligned} \tag{F.3}$$

Making the replacement $s \to su$ and $t \to tu$ and integrating over u, we obtain

$$\begin{aligned} I_A^{(\alpha)} &= \left(\int_q \mathrm{e}^{-q^2}\right)^2 m^{-2\epsilon}\frac{\Gamma(\epsilon)}{\Gamma(\alpha)\Gamma(\frac{\alpha}{2})^2} \\ &\quad\times \int_{s,t>0} \frac{s^{\frac{\alpha}{2}-1}t^{\alpha-1}}{(st+s+t)^{\alpha}}(st+s+t)^{\frac{\epsilon}{2}}(1+s+t)^{-\epsilon} \\ &= \left(\int_q \mathrm{e}^{-q^2}\right)^2 m^{-2\epsilon}\frac{\Gamma(\epsilon)}{\Gamma(\alpha)\Gamma(\frac{\alpha}{2})^2}\left(J_1+J_2+J_3+O(\epsilon)\right) \end{aligned} \tag{F.4}$$

$$J_1 = \int_0^1 \mathrm{d}t \int_0^\infty \mathrm{d}s\, \frac{s^{\frac{\alpha}{2}-1}t^{\alpha-1}}{(st+s+t)^{\alpha}} \tag{F.5}$$

$$J_2 = \int_1^\infty \mathrm{d}t \int_0^\infty \mathrm{d}s\, s^{\frac{\alpha}{2}-1}t^{\alpha-1} \times \left[(st+s+t)^{-\alpha} - (1+s)^{-\alpha}t^{-\alpha}\right] \tag{F.6}$$

$$\begin{aligned} J_3 &= \int_1^\infty \mathrm{d}t \int_0^\infty \mathrm{d}s\, s^{\frac{\alpha}{2}-1}(1+s)^{\frac{\epsilon}{2}-\alpha}t^{-1-\frac{\epsilon}{2}} \\ &= \frac{2}{\epsilon}\frac{\Gamma(\frac{\alpha}{2})\Gamma(\frac{\alpha-\epsilon}{2})}{\Gamma(\alpha-\frac{\epsilon}{2})} \end{aligned} \tag{F.7}$$

J_1 and J_2 are now both integrated over s. Changing in J_2 the integration over t to that over $1/t$, we obtain

$$J_1 + J_2 = 2^{1-\alpha}\sqrt{\pi}\,\frac{\Gamma(\frac{\alpha}{2})}{\Gamma(\frac{1+\alpha}{2})}\int_0^1 \mathrm{d}t\,\frac{1+t^{\frac{\alpha}{2}}-(1+t)^{\frac{\alpha}{2}}}{t(1+t)^{\frac{\alpha}{2}}} \tag{F.8}$$

$$(J_1+J_2)\big|_{\alpha=1} = 0 \tag{F.9}$$

$$(J_1+J_2)\big|_{\alpha=1} = 2\pi\ln 2\,. \tag{F.10}$$

Putting everything together, the final result is

$$\begin{aligned} I_A^{(\alpha)} &= \left[\frac{1}{2\epsilon^2}+\frac{1}{4\epsilon}\left(\int_0^1 \mathrm{d}t\,\frac{1+t^{\frac{\alpha}{2}}-(1+t)^{\frac{\alpha}{2}}}{t(1+t)^{\frac{\alpha}{2}}}\right.\right. \\ &\qquad\left.\left.+\frac{\Gamma'(a)}{\Gamma(a)}-\frac{\Gamma'(\frac{a}{2})}{\Gamma(\frac{a}{2})}\right)\right]\left(\epsilon I_1^{(\alpha)}\right)^2+O(\epsilon^0) \end{aligned} \tag{F.11}$$

$$I_A^{(1)} = \left[\frac{1}{2\epsilon^2}+\frac{\ln 2}{\epsilon}\right]\left(\epsilon I_1^{(\alpha)}\right)^2+O(\epsilon^0) \tag{F.12}$$

$$I_A^{(2)} = \left[\frac{1}{2\epsilon^2}+\frac{1}{4\epsilon}\right]\left(\epsilon I_1^{(\alpha)}\right)^2+O(\epsilon^0)\,. \tag{F.13}$$

APPENDIX G: CALCULATION OF THE INTEGRAL I_η^α

The calculations for the corrections to friction are the same as with short-range elasticity, except that the integrals I_1, I_A and I_η change. The first two have already been calculated in appendix F. We now attack the masterpiece, $I_\eta^{(\alpha)}$. For simplicity, we restrict ourselves to $\alpha = 1$.

$$I_\eta^{(1)} := \int\limits_{q_1,q_2} \frac{1}{(q_1^2+m^2)^{\frac{1}{2}}\,(q_2^2+m^2)\,[(q_2^2+m^2)^{\frac{1}{2}}+(q_3^2+m^2)^{\frac{1}{2}}]} \tag{G.1}$$

Using:

$$\mathrm{e}^{-\sqrt{x}} = \frac{1}{2\sqrt{\pi}}\int_0^\infty \mathrm{d}s\, s^{-3/2}\mathrm{e}^{-\frac{1}{4s}}\mathrm{e}^{-sx} \tag{G.2}$$

we have

$$\begin{aligned} \frac{1}{\sqrt{a}+\sqrt{b}} &= \int_{t_3>0} \mathrm{e}^{-t_3(\sqrt{a}+\sqrt{b})} \\ &= \frac{1}{4\pi}\int\limits_{t_3,s_1,s_2>0} (s_1s_2)^{-\frac{3}{2}}\mathrm{e}^{-\frac{1}{4s_1}-\frac{1}{4s_2}}\mathrm{e}^{-s_1t_3^2a-s_2t_3^2b} \end{aligned} \tag{G.3}$$

With the help of (G.3), we can write $I_\eta^{(1)}$ as

$$\begin{aligned} I_\eta^{(1)} &= \frac{1}{4\pi}\frac{1}{\Gamma(\frac{1}{2})}\int\limits_{q_1,q_2}\int\limits_{t_1,t_2,t_3,s_1,s_2>0} t_1^{-\frac{1}{2}}(s_1s_2)^{-\frac{3}{2}}\,\mathrm{e}^{-t_1(q_1^2+m^2)-(t_2+s_1t_3^2)(q_2^2+m^2)-s_2t_3^2(q_3^2+m^2)}\,\mathrm{e}^{-\frac{1}{4s_1}-\frac{1}{4s_2}} \\ &= \frac{1}{4\pi}\frac{1}{\Gamma(\frac{1}{2})}\left(\int_q \mathrm{e}^{-q^2}\right)^2\int\limits_{t_1,t_2,t_3,s_1,s_2>0}\frac{t_1^{-\frac{1}{2}}(s_1s_2)^{-\frac{3}{2}}\,\mathrm{e}^{-m^2(t_1+t_2+(s_1+s_2)t_3^2)}\,\mathrm{e}^{-\frac{1}{4s_1}-\frac{1}{4s_2}}}{(t_1t_2+s_1s_2t_3^4+(s_1+s_2)t_1t_3^2+s_2t_2t_3^2)^{1-\frac{\epsilon}{2}}} \end{aligned}$$

$$= \frac{1}{4\pi}\frac{1}{\Gamma(\frac{1}{2})}\left(\int_q \mathrm{e}^{-q^2}\right)^2 \int\limits_{t_1,t_2,t_3,s_1,s_2>0} t_3^{-1+2\epsilon}\,\frac{t_1^{-\frac{1}{2}}(s_1s_2)^{-\frac{3}{2}}\,\mathrm{e}^{-m^2t_3^2(t_1+t_2+s_1+s_2)}\,\mathrm{e}^{-\frac{1}{4s_1}-\frac{1}{4s_2}}}{(t_1t_2+s_1s_2+(s_1+s_2)t_1+s_2t_2)^{1-\frac{\epsilon}{2}}}$$

$$= \frac{1}{4\pi}\frac{1}{\Gamma(\frac{1}{2})}\left(\int_q \mathrm{e}^{-q^2}\right)^2 \frac{\Gamma(\epsilon)}{2}\,m^{-2\epsilon} \int\limits_{t_1,t_2,s_1,s_2>0} \frac{t_1^{-\frac{1}{2}}(s_1s_2)^{-\frac{3}{2}}\,\mathrm{e}^{-\frac{1}{4s_1}-\frac{1}{4s_2}}}{(t_1t_2+s_1s_2+(s_1+s_2)t_1+s_2t_2)^{1-\frac{\epsilon}{2}}(t_1+t_2+s_1+s_2)^{\epsilon}}$$

$$= \frac{1}{4\pi}\frac{1}{\Gamma(\frac{1}{2})}\left(\int_q \mathrm{e}^{-q^2}\right)^2 \frac{\Gamma(\epsilon)}{2}\,m^{-2\epsilon}J\,. \tag{G.4}$$

In the third line we have made the replacement $t_1 \to t_3^2 t_1$ and $t_2 \to t_3^2 t_2$. In the fourth line we have integrated over t_3. The integral J is again decomposed in converging parts (which can be evaluated at $\epsilon = 0$) and parts that can be integrated analytically:

$$J = J_1 + J_2 + J_3 + O(\epsilon) \tag{G.5}$$

$$J_1 = \int_{t_1,s_1,s_2>0} t_1^{-\frac{1}{2}}(s_1s_2)^{-\frac{3}{2}}\mathrm{e}^{-\frac{1}{4s_1}-\frac{1}{4s_2}} \int_{t_2>1} \frac{1}{t_1t_2+s_1s_2+(s_1+s_2)t_1+s_2t_2} - \frac{1}{t_2(s_2+t_1)} \tag{G.6}$$

$$J_2 = \int_{t_1,s_1,s_2>0} t_1^{-\frac{1}{2}}(s_1s_2)^{-\frac{3}{2}}\mathrm{e}^{-\frac{1}{4s_1}-\frac{1}{4s_2}} \int_{0<t_2<1} \frac{1}{t_1t_2+s_1s_2+(s_1+s_2)t_1+s_2t_2} \tag{G.7}$$

$$J_3 = \int_{t_1,s_1,s_2>0} t_1^{-\frac{1}{2}}(s_1s_2)^{-\frac{3}{2}}\mathrm{e}^{-\frac{1}{4s_1}-\frac{1}{4s_2}} \int_{t_2>1} t_2^{-1-\frac{\epsilon}{2}}(s_2+t_1)^{-1+\frac{\epsilon}{2}}\,. \tag{G.8}$$

Integrating in J_3 over t_2, t_1, s_1 and s_2 (in this order) we find

$$J_3 = 2^{-\epsilon}\frac{16\pi}{\epsilon}\,\Gamma\left(\frac{1-\epsilon}{2}\right)\,. \tag{G.9}$$

In order to calculate J_1 and J_2, it is convenient to do the integration over t_2 in both integrals first. Taking the sum, some terms cancel:

$$J_1 + J_2 = \int_{t_1,s_1,s_2>0} t_1^{-\frac{1}{2}}(s_1s_2)^{-\frac{3}{2}}\mathrm{e}^{-\frac{1}{4s_1}-\frac{1}{4s_2}}\,\frac{\ln(s_2+t_1)-\ln(s_1s_2+t_1(s_1+s_2))}{s_2+t_1}\,. \tag{G.10}$$

The logarithms have to be written as derivatives:

$$J_1 + J_2 = \left.\frac{\partial}{\partial b}\right|_{b=0} \int_{t_1,s_1,s_2>0} t_1^{-\frac{1}{2}}(s_1s_2)^{-\frac{3}{2}}\mathrm{e}^{-\frac{1}{4s_1}-\frac{1}{4s_2}}\Big((s_2+t_1)^{-1+b} - (s_2+t_1)^{-1}(s_1s_2+t_1(s_1+s_2))^b\Big)\,. \tag{G.11}$$

Making the change of variables $s_1 \to 1/s_1$, $s_2 \to 1/s_2$, $t_1 \to t_1/s_2$ and $s_1 \to s_1s_2$ (in this order), we obtain

$$J_1 + J_2 = \left.\frac{\partial}{\partial b}\right|_{b=0} \int_{t_1,s_1,s_2>0} s_1^{-\frac{1}{2}}s_2^{\frac{1}{2}-b}t_1^{-\frac{1}{2}}\Big((1+t_1)^{-1+b} - (1+t_1)^{-1}s_1^{-b}s_2^{-b}(1+t_1(1+s_1))^b\Big)\,\mathrm{e}^{-\frac{1}{4}s_2(1+s_1)}\,. \tag{G.12}$$

The integration over s_2 can now be done analytically:

$$J_1 + J_2 = \left.\frac{\partial}{\partial b}\right|_{b=0} \int_{t_1,s_1} s_1^{-\frac{1}{2}}t_1^{-\frac{1}{2}}\left[\frac{\Gamma\left(\frac{3}{2}-b\right)}{(1+t_1)^{1-b}}\left(\frac{1+s_1}{4}\right)^{b-\frac{3}{2}} - \frac{\Gamma\left(\frac{3}{2}-2b\right)(1+t_1(1+s_1))^b}{(1+t_1)s_1^b}\left(\frac{1+s_1}{4}\right)^{2b-\frac{3}{2}}\right]\,. \tag{G.13}$$

In order to proceed, we split these integrals as follows

$$J_1 + J_2 = K_1 + K_2 + K_3 \tag{G.14}$$

$$K_1 = \left.\frac{\partial}{\partial b}\right|_{b=0} \int_{t_1,s_1} s_1^{-\frac{1}{2}}t_1^{-\frac{1}{2}}\frac{\Gamma\left(\frac{3}{2}-b\right)}{(1+t_1)^{1-b}}\left(\frac{1+s_1}{4}\right)^{b-\frac{3}{2}} = \left.\frac{\partial}{\partial b}\right|_{b=0} 8\,\pi\,4^{-b}\,\Gamma\left(\tfrac{1}{2}-b\right) \tag{G.15}$$

$$K_2 = -\left.\frac{\partial}{\partial b}\right|_{b=0} \int_{t_1,s_1} s_1^{-\frac{1}{2}}t_1^{-\frac{1}{2}}\frac{\Gamma\left(\frac{3}{2}-2b\right)}{(1+t_1)s_1^b}\left(\frac{1+s_1}{4}\right)^{2b-\frac{3}{2}} = -\left.\frac{\partial}{\partial b}\right|_{b=0} 8\,\pi^{\frac{3}{2}}\,4^{-b}\,\Gamma\left(1-2b\right) \tag{G.16}$$

$$K_3 = -\left.\frac{\partial}{\partial b}\right|_{b=0} \int_{t_1,s_1} s_1^{-\frac{1}{2}}t_1^{-\frac{1}{2}}\frac{\Gamma\left(\frac{3}{2}\right)(1+t_1(1+s_1))^b}{(1+t_1)}\left(\frac{1+s_1}{4}\right)^{-\frac{3}{2}} \tag{G.17}$$

To evaluate K_3 one first has to take the derivative:

$$K_3 = -8\,\Gamma\left(\tfrac{3}{2}\right)\int_{t_1,s_1} \frac{\ln(1+t_1(1+s_1))}{\sqrt{s_1}\,\sqrt{t_1}\,(1+t_1)\,(1+s_1)^{\frac{3}{2}}}\,. \tag{G.18}$$

Integrating first over t_1 and then s_1 gives

$$K_3 = -4\pi^{\frac{3}{2}}\int_{s_1} \frac{2\,\mathrm{atanh}(1/\sqrt{1+s_1})+\ln(s_1)}{\sqrt{s_1}\,(1+s_1)^{\frac{3}{2}}}$$

$$= 8\pi^{\frac{3}{2}} \left(2\ln -2\pi\right) \ . \tag{G.19}$$

Putting everything together his gives finally

$$I_\eta^{(1)} = \left(\frac{1}{2\epsilon^2} + \frac{\ln 2 - \frac{\pi}{4}}{\epsilon}\right) (\epsilon I_1^{(1)})^2 + \text{finite} \ . \tag{G.20}$$

APPENDIX H: FIXED-POINT FUNCTION AT SECOND ORDER

In this appendix, we show how to obtain the fixed-point function for $\Delta(u)$ at second order. We restrict the discussion to $\alpha = 2$. We use the notations of equation (IV.5). First, one needs the 1-loop function $y_1(u)$ both by solving (IV.11) numerically and as a Taylor-series about 0. The latter is obtained by deriving the 1-loop β-function at the origin and fitting the coefficients as

$$\begin{aligned} y_1(u) = 1 - u + \frac{u^2}{3} - \frac{u^3}{36} - \frac{u^4}{270} - \frac{u^5}{4320} + \frac{u^6}{17010} \\ + \frac{139u^7}{5443200} + \frac{u^8}{204120} + \frac{571u^9}{2351462400} \\ - \frac{281u^{10}}{1515591000} - \frac{163879u^{11}}{2172751257600} \\ - \frac{5221u^{12}}{354648294000} - \frac{5246819u^{13}}{10168475885568000} \\ + \frac{5459u^{14}}{7447614174000} + \frac{534703531u^{15}}{1830325659402240000} \cdots \end{aligned} \tag{H.1}$$

The β-function at second order yields a linear differential equation for $y_2(u)$. It is numerically singular at small u. Therefore one has to expand it in a Taylor-series about 0. Using the above information and the knowledge of ζ_2, one finds

$$\begin{aligned} y_2(u) = -1.14012\, u + 0.967798\, u^2 - 0.202495\, u^3 \\ -0.019299\, u^4 + 0.00259234\, u^5 + 0.0015302\, u^6 \\ +0.000286423\, u^7 - 6.25533\, 10^{-6}\, u^8 \\ -0.0000206648\, u^9 - 6.48801\, 10^{-6}\, u^{10} \\ -7.85669\, 10^{-7}\, u^{11} + 1.88404\, 10^{-7}\, u^{12} \\ +1.24668\, 10^{-7}\, u^{13} + 3.13093\, 10^{-8}\, u^{14} + \ldots \end{aligned} \tag{H.2}$$

The differential equation for $y_2(u)$ is then solved numerically, starting at $u \approx 0.5$. By integrating from that point both towards 0 and towards infinity, one verifies that Taylor-expansion and numerically obtained curve coincide in their respective domain of validity. This is shown on figure H.1. One also verifies that the numerically obtained function converges to 0 for large u, thus the exponent ζ_2 obtained above is correct.

It is a good question to ask for how large ϵ the fixed-point function $\Delta(u) = \frac{\epsilon}{3} y_1(u) + \frac{\epsilon^2}{18} y_2(u)$ might be a good approximation for the true disorder correlator. Let us note that if one demands that $\Delta(u) > 0$, thus that forces be never anti-correlated, this is only satisfied if

$$\epsilon < \epsilon_c \approx 1.6 \ . \tag{H.3}$$

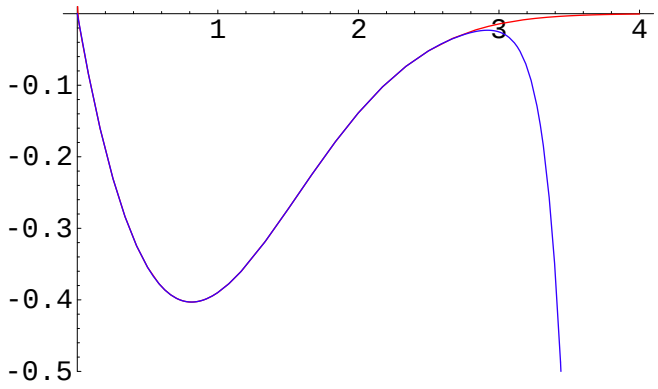


FIG. H.1: The fixed-point function of the RG-flow $y_2(u)$ at second order in ϵ. Upper curve: Numerical integration. Lower curve: Taylor-expansion about 0.

APPENDIX I: STABILITY OF THE FIXED POINTS

We now consider the stability of the periodic fixed point given in (IV.33). Define $K[f]$ as

$$K[f] := \lim_{\kappa \to 0} \frac{1}{\kappa} \left[\beta(\Delta^*(u) + \kappa f(u)) - \beta(\Delta^*(u))\right] \ . \tag{I.1}$$

The eigenfunctions and eigenvalues are

$$K[f] = \lambda f \ . \tag{I.2}$$

We find the following solutions (with $x = u(1-u)$ and normalized to $f(0) = 1$)

$$
\begin{aligned}
&\lambda_1 = \epsilon\ , && f_1 = 1\\
&\lambda_2 = -\epsilon - \tfrac{7}{3}\epsilon^2\ , && f_2 = 1-(6+4\epsilon)x\\
&\lambda_3 = -4\epsilon - 5\epsilon^2\ , && f_3 = 1-(15+20\epsilon)x+(45+85\epsilon)x^2\\
&\lambda_4 = \tfrac{-25\epsilon}{3} - \tfrac{140\epsilon^2}{9}\ , && f_4 = 1-(28+\tfrac{238\epsilon}{3})x+(\tfrac{616}{3}+\tfrac{23548\epsilon}{27})x^2-(\tfrac{4004}{9}+\tfrac{185402\epsilon}{81})x^3\\
&\lambda_5 = -14\epsilon - 35\epsilon^2\ , && f_5 = 1-(45+225\epsilon)x+(585+4500\epsilon)x^2-(2925+\tfrac{110475\epsilon}{4})x^3+(\tfrac{9945}{2}+\tfrac{424755\epsilon}{8})x^4\\
&\lambda_6 = -21\epsilon - 66\epsilon^2\ , && f_6 = 1-(66+517\epsilon)x+(1320+16148\epsilon)x^2-(11220+169928\epsilon)x^3+(42636+\tfrac{3672944\epsilon}{5})x^4\\
& && \quad -(\tfrac{298452}{5}+\tfrac{280555588\epsilon}{25})x^5
\end{aligned}
\tag{I.3}
$$

This shows that apart from the constant mode (the shift) discussed in the text, the fixed point is stable.

APPENDIX J: CALCULATION OF CORRELATION FUNCTIONS

In this Appendix we show how to compute a correlation function in the renormalized theory. As an example we study the periodic case, i.e. we compute the amplitude A_d in (IV.40). To do that we assume that we are exactly at the fixed point.

The correlation function is time-independent, as was shown in Section (III D), and takes the scaling form:

$$\langle u_q u_{-q}\rangle_{\rm nl} = \frac{1}{\epsilon\tilde{I}_1}\Delta^*(0) m^{-d} F_d\left(\frac{q}{m}\right)\ , \tag{J.1}$$

where we have restored the factor previously absorbed in Δ. The scaling function is universal and satisfies $F(0)=1$ since our calculation was performed at zero external momenta in presence of a mass and $F(z)\sim B/z^d$ at large z. In $d=4$ one has $F_4(z)=1/(1+z^2)^2$. We want to obtain the scaling function to the next order; in particular to compute A_d we need $B=1+b\epsilon+O(\epsilon^2)$. The universal amplitude reads:

$$
\begin{aligned}
A_d &= \frac{2S_d}{(2\pi)^d\epsilon\tilde{I}_1} B\Delta^*(0) \qquad (J.2)\\
&= (1+b\epsilon)(2+\epsilon)\left(\frac{\epsilon}{36}+\frac{\epsilon^2 X^{(\alpha)}}{108}\right)+O(\epsilon^3)\ ,
\end{aligned}
$$

which yields:

$$A_d = \frac{1}{18}\epsilon + \frac{2X^{(\alpha)}+3+6b}{108}\epsilon^2\ . \tag{J.3}$$

Computing b requires computing diagrams with external momentum which we do now. Let us use straight perturbation theory with Δ_0, as in Section (III C 1). One has

$$(q^2+m^2)^2\langle u_q u_{-q}\rangle = \Delta_0(0) - \Delta_0'(0^+)^2 I(q) \tag{J.4}$$

$$I(q) = \int_p \frac{1}{(p^2+m^2)((p+q)^2+m^2)}\ . \tag{J.5}$$

Let us reexpress this by the renormalized dimensionless disorder given in (III.35) and (III.18) at $u=0$:

$$\Delta_0(0) = m^\epsilon(\Delta(0)+\Delta'(0^+)^2 m^\epsilon I(0))\ . \tag{J.6}$$

This gives:

$$
\begin{aligned}
&(q^2+m^2)^2\langle u_q u_{-q}\rangle\\
&\quad = m^\epsilon(\Delta(0)-\Delta'(0^+)^2 m^\epsilon(I(q)-I(0)))\\
&\quad = m^\epsilon\frac{1}{\epsilon\tilde{I}_1}\Delta^*(0)(1-\epsilon\frac{1}{\epsilon\tilde{I}_1}m^\epsilon(I(q)-I(0)))\ , \qquad (J.7)
\end{aligned}
$$

where we have reestablished the factor $\Delta(u)=\frac{1}{\epsilon\tilde{I}_1}\Delta^*(u)$ and used the fixed point condition $\Delta^{*\prime}(0^+)^2=\epsilon\Delta^*(0)$ This substitution acts as a counter-term which exactly subtract the divergence as it should. The result is finite. Using that:

$$
\begin{aligned}
I(q) &= \int_p\int_{s,t>0} {\rm e}^{-s(p+q/2)^2-t(p-q/2)^2-(s+t)m^2}\\
&= \int_p {\rm e}^{-p^2}\int_{s,t>0}(s+t)^{-d/2}{\rm e}^{-q^2\frac{st}{s+t}-(s+t)m^2}\\
&= \int_p {\rm e}^{-p^2} m^{-\epsilon}\Gamma\left(2-\frac{d}{2}\right)\\
&\quad\times\int_{t>0}(1+t)^{-d/2}\left[(1+t)+\frac{t}{1+t}\frac{q^2}{m^2}\right]^{-\epsilon/2}\ . \qquad (J.8)
\end{aligned}
$$

One obtains the scaling function in the form ($z=|q|/m$):

$$
\begin{aligned}
F_d(z) &= \frac{1}{(1+z^2)^2}\left\{1-\int_0^\infty {\rm d}t\,\frac{1}{(1+t)^2}\left[\left(1+\frac{tz^2}{(1+t)^2}\right)^{-\epsilon/2}-1\right]\right\} \qquad (J.9)\\
&= \frac{1}{(1+z^2)^2}\left\{1+\frac{\epsilon}{2}\int_0^1 {\rm d}s\,\ln(1+z^2(s-s^2))\right\}+O(\epsilon^2)
\end{aligned}
$$

$$= \frac{1}{(1+z^2)^2}\left\{1+\frac{\epsilon}{2}\left[-2+\sqrt{\frac{4+z^2}{z^2}}\left(\ln 2-\ln\left(2+z^2-z\sqrt{4+z^2}\right)\right)\right]\right\}+O(\epsilon^2)$$
$$\stackrel{\zeta\to\infty}{\longrightarrow} \frac{1}{z^4}\left\{1+\frac{\epsilon}{2}\left[-2+2\ln z\right]\right\}+\mathcal{O}(\epsilon^2)$$

We want to match at large z:

$$F_d(z) = \frac{1}{z^4}(1+b\epsilon)z^\epsilon = \frac{1}{z^4}(1+\epsilon(\ln z+b)+O(\epsilon^2)) \quad \text{(J.10)}$$

The above result yields

$$b = -1\ . \quad \text{(J.11)}$$

APPENDIX K: ANOMALOUS AND NON-ODD GRAPHS

In this Appendix we write all anomalous 2-loop graphs contributing to the correction of a non-analytic disorder. In a first step we make no assumption and give their general expressions: Already at that stage some cancellations are apparent. In a second step we consider the limit $v \to 0^+$ at $T = 0$. We check all cancellations given in the text and show that no additional singularities occur. The multiplicity factors are included in the given expressions. Of course since we want only corrections to disorder we will give only the expressions when the separations of the times between the two external response fields are much larger than the separations within each connected component. If this were not the case, as is needed e.g. in the calculation of a 2-point correlation function to order Δ^3, the above expressions should be reexamined separately. Equivalently, the expressions given here are correct only for $u > 0$ and may become incorrect at $u = 0$.

Graphs which are odd need not be considered (see main text). Each remaining graph, e.g. c_i is written in the shorthand notation form:

$$\text{graph } \mathrm{c}_i = \int_{x,y}\int_{t_i>0} F_{\mathrm{c}}\mathrm{c}_i\ . \quad \text{(K.1)}$$

The only anomalous non-vanishing graphs of class A are:

$$F_{\mathrm{c}} = R_{yt_1}R_{yt_2}R_{x-yt_3}R_{xt_4} \quad \text{(K.2)}$$
$$\mathrm{c}_1 = 2\langle\Delta'(u^x_0-u^x_{-t_3-t_2-t_4})\Delta'(u^y_{-t_3}-u^y_{-t_3-t_2-t_1})\rangle\Delta''(u) \quad \text{(K.3)}$$
$$\mathrm{c}_2 = 2\langle\Delta(u^x_{-t_4}-u^x_{-t_2-t_3})\Delta''(u^y_0-u^y_{-t_2-t_1})\rangle\Delta''(u) \quad \text{(K.4)}$$
$$\mathrm{c}_4 = 2\Delta'(u^x_0-u^x_{-t_2-t_3-t_4})\Delta'(u^y_{-t_4-t_2}-u^y_{-t_4-t_1})\Delta''(u) \quad \text{(K.5)}$$
$$\mathrm{c}_5 = -2\Delta(u^x_{-t_1-t_2-t_3}-u^x_{-t_1-t_4})\Delta''(u^y_0-u^y_{-t_2-t_1})\Delta''(u) \quad \text{(K.6)}$$
$$F_{\mathrm{e}} = F_{\mathrm{f}} = R_{x-yt_1}R_{x-yt_2}R_{xt_3}R_{yt_4} \quad \text{(K.7)}$$
$$\mathrm{e}_1 = \Delta''(u)\langle\Delta'(u^x_{-t_3}-u^x_{-t_1-t_4})\Delta'(u^y_{-t_4}-u^y_{-t_3-t_2})\rangle \quad \text{(K.8)}$$
$$\mathrm{f}_2 = 2\Delta''(u)\langle\Delta'(u^x_{-t_3}-u^x_{-t_3-t_2-t_1})\Delta'(u^y_{-t_2-t_3}-u^y_{-t_4})\rangle\ . \quad \text{(K.9)}$$

For the graphs d one easily sees that the following relations are exact (with no other assumption than $u \neq 0$):

$$F_{\mathrm{c}} = F_{\mathrm{d}} = R_{yt_1}R_{yt_2}R_{x-yt_3}R_{xt_4} \quad \text{(K.10)}$$
$$\mathrm{d}_2+\mathrm{d}_4 = 0 \quad \text{(K.11)}$$
$$\mathrm{d}_6+\mathrm{d}_8 = 0\ . \quad \text{(K.12)}$$

The only anomalous non-vanishing graphs of class B are:

$$F_{\mathrm{k}} = F_{\mathrm{l}} = R_{xt_1}R_{xt_2}R_{y-xt_3}R_{y-xt_4} \quad \text{(K.13)}$$
$$\mathrm{k}_1 = c\Delta''(u)\langle\Delta''(u^x_{-t_2}-u^x_{-t_1})\Delta(u^y_{-t_2-t_4}-u^y_{-t_1-t_3})\rangle \quad \text{(K.14)}$$
$$\mathrm{l}_1 = -c\Delta''(u)\langle\Delta''(u^x_{-t_2}-u^x_{-t_1})\Delta(u^y_{-t_1-t_4}-u^y_{-t_1-t_3})\rangle \quad \text{(K.15)}$$
$$F_{\mathrm{i}} = R_{xt_1}R_{xt_2}R_{yt_3}R_{yt_4} \quad \text{(K.16)}$$
$$\mathrm{i}_3 = -\Delta''(u)\langle\Delta'(u^x_0-u^x_{-t_1-t_2})\Delta'(u^y_0-u^y_{-t_3-t_4})\rangle\ . \quad \text{(K.17)}$$

All graphs of class C exactly vanish. For instance:

$$\mathrm{m}_2 = \Delta(0)\Delta'''(u_0-u_{-t_3})\Delta'(u) \quad \text{(K.18)}$$
$$\mathrm{n}_2 = -\Delta(0)\Delta'''(u_0-u_{-t_3})\Delta'(u)\ . \quad \text{(K.19)}$$

We now evaluate these graphs in the quasi-static depinning limit, substituting $\Delta(u)$ by its power series as a function of u, as explained in the main text. We need in addition to (II.9):

$$\Delta'(u) = \Delta'(0^+)\mathrm{sgn}(u)+\Delta''(0^+)u+\dots$$
$$\Delta''(u) = 2\Delta'(0^+)\delta(u)+\Delta''(0^+)+\dots\ . \quad \text{(K.20)}$$

In $\Delta''(u)$ evaluated at zero we have written the δ-function which may in principle be needed. If this were the case that would pose two unpleasant problems: Firstly a different viewpoint were to argue that $\Delta''(u)$ should simply be continued to zero which does not pose any problem since it is pair. Second it would open the possibility to problematic singular terms ($\delta(v)$ or $1/v$) as $v \to 0^+$. Fortunately, in all our 2-loop calculations this never happens: these δ-functions, if put by hand, cancel. This confirms that, at least to this order, no pathology arises.

Let us start with the sum $c_2 + c_5$. Using (II.9) and (K.20) one sees that the term proportional to $\Delta(0)\Delta''(0^+)$ cancels. Let us test the δ-function. Then one needs to go one order further in the expansion of the Δ term since averages of the type $\delta(u_1)u_2$ have dimension one, similar to $\langle\mathrm{sgn}(u_1)\mathrm{sgn}(u_2)\rangle$, and can thus yield a non-zero result at zero temperature (higher order terms yielding dimensions as positive powers of the field are not needed as they vanish at zero T). This yields

$$c_2 + c_5 = 4\Delta'(0^+)^2\Delta''(u)\langle(|u^x_{-t_4} - u^x_{-t_2-t_3}| - |u^x_{-t_1-t_2-t_3} - u^x_{-t_1-t_4}|)\delta(u^y_0 - u^y_{-t_2-t_1})\rangle \ , \tag{K.21}$$

which strictly vanish upon the replacement $u^x_t - u^x_{t'} \to v(t-t')$. This is fortunate since this term would have led to a $1/v$ singularity. Note that all diagrams $a-g$ in the 2-loop correction to η could a priori suffer from the same problem since Δ'' functions must be expanded. However one notes that their arguments are always strictly positive in the depinning limit, which avoids, as it did here, the problem. Similarly one has

$$c_4 = 2\Delta'(0^+)^2\Delta''(u)\langle \mathrm{sgn}(u^x_0 - u^x_{-t_2-t_3-t_4})\mathrm{sgn}(u^y_{-t_4-t_2} - u^y_{-t_4-t_1})\rangle \ . \tag{K.22}$$

Performing the replacement $u^x_t - u^x_{t'} \to v(t-t')$, since the $t_i > 0$ and because F_c is symmetric in $t_1 \leftrightarrow t_2$ one finds that

$$c_2 + c_5 = c_4 = 0 \tag{K.23}$$

at depinning. Note that these cancellations do not happen any longer, if the field is not a monotonic function, a question which will be discussed in Ref.[34].

A similar calculation shows that at depinning one has also:

$$k_1 + l_1 = 0 \ . \tag{K.24}$$

There, in the singular part, the δ-function implies that $t_1 = t_2$ yielding the cancellation via a slightly different mechanism than above.

Finally we are left with the only non-zero anomalous non-trivial graphs c_1, e_1, f_2 and i_1 to compute, which is done in the text.

ACKNOWLEDGMENTS

It is a pleasure to thank E. Bouchaud, E. Brézin, J. Ferré, W. Krauth, S. Lemerle, E. Rolley and A. Rosso for stimulating discussions.

[1] M. Kardar, *Nonequilibrium dynamics of interfaces and lines*, Phys. Rep. **301** (1998) 85–112.

[2] D.S. Fisher, *Collective transport in random media: from superconductors to earthquakes*, Phys. Rep. **301** (1998) 113–150.

[3] G. Blatter, M.V. Feigel'man, V.B. Geshkenbein, A.I. Larkin and V.M. Vinokur, *Vortices in high-temperature superconductors*, Rev. Mod. Phys. **66** (1994) 1125.

[4] M. Chandran, R. T. Scalettar and G.T. Zimanyi, *Metastabilty and uniqueness of vortex states at depinning*, cond-mat/**0204039** (2002).

[5] G. Bertotti, *Hysteresis and Magnetism*, Academic Press, 1998.

[6] T. Nattermann, *Theory of the random field Ising model*, in A.P. Young, editor, *Spin glasses and random fields*, World Scientific, Singapore, 1997.

[7] S. Zapperi and M. Zaiser, *Depinning of a dislocation: the influence of long-range interactions*, Materials Science and Engineering **A309-A310** (2000) 348–51.

[8] G. Gruner, *The dynamics of charge-density waves*, Rev. of Mod. Phys. **60** (1988) 1129–81.

[9] A.A. Middleton and D.S. Fisher, *Critical behavior of charge-density waves below threshold: numerical and scaling analysis*, Phys. Rev. B **47** (1993) 3530–52.

[10] T. Giamarchi and P. Le Doussal, *Elastic theory of flux lattices in the presence of weak disorder*, Phys. Rev. B **52** (1995) 1242–70.

[11] T. Giamarchi and P. Le Doussal, *Statics and dynamics of disordered elastic systems*, in A.P. Young, editor, *Spin glasses and random fields*, World Scientific, Singapore, 1997.

[12] A. Prevost, PhD thesis, Orsay, 1999.

[13] A. Prevost, E. Rolley and C. Guthmann, *Thermally activated motion of the contact line of a liquid ^{4}He meniscus on a cesium substrate*, Phys. Rev. Lett. **83** (1999) 348–51.

[14] D. Ertas and M. Kardar, *Anisotropic scaling in threshold critical dynamics of driven directed lines*, Phys. Rev. **B 53** (1996) 3520–42.

[15] J. Schmittbuhl and K.J. Maloy, *Direct observation of a self-affine crack propagation*, Phys. Rev. Lett. **78** (1997) 3888–91.

[16] D.S. Fisher, *Sliding charge-density waves as a dynamical critical phenomena*, Phys. Rev. **B 31** (1985) 1396–1427.

[17] O. Narayan and D.S. Fisher, *Critical behavior of sliding charge-density waves in 4- epsilon dimensions*, Phys. Rev. B **46** (1992) 11520–49.

[18] J. Vannimenus and B. Derrida, *A solvable model of interface depinning in random media*, J. Stat. Phys. **105** (2001) 1–23.

[19] T. Nattermann, S. Stepanow, L.-H. Tang and H. Leschhorn, *Dynamics of interface depinning in a disordered medium*, J. Phys. II (France) **2** (1992) 1483–8.

[20] H. Leschhorn, T. Nattermann, S. Stepanow and L.-H. Tang, *Driven interface depinning in a disordered medium*, Annalen der Physik **6** (1997) 1–34.

[21] O. Narayan and D.S. Fisher, *Threshold critical dynamics of driven interfaces in random media*, Phys. Rev. B **48** (1993) 7030–42.

[22] D.S. Fisher, *Interface fluctuations in disordered systems: $5-\epsilon$ expansion*, Phys. Rev. Lett. **56** (1986) 1964–97.

[23] K.B. Efetov and A. I. Larkin, Sov. Phys. JETP **45** (1977) 1236.

[24] A. Aharony, Y. Imry and S.K. Ma, *Lowering of dimensionality in phase transitions with random fields*, Phys. Rev. Lett. **37** (1976) 1364–7.

[25] G. Grinstein, *Ferromagnetic phase transitions in random fields: the breakdown of scaling laws*, Phys. Rev. Lett. **37** (1976) 944–7.

[26] G. Parisi and N. Sourlas, *Random magnetic fields, supersymmetry, and negative dimensions*, Phys. Rev. Lett. **43** (1979) 744–5.

[27] J.L. Cardy, *Nonperturbative effects in a scalar supersymmetric theory*, Phys. Lett. **125 B** (1983) 470–2.

[28] P. Chauve, T. Giamarchi and P. Le Doussal, *Creep and depinning*

in disordered media, Phys. Rev. B **62** (2000) 6241–67.
[29] H. Bucheli, O.S. Wagner, V.B. Geshkenbein, A.I. Larkin and G. Blatter, *$(4+n)$-dimensional elastic manifolds in random media: a renormalization-group analysis*, Phys. Rev. B **57** (1998) 7642–52.
[30] O.S. Wagner, V.B. Geshkenbein, A.I. Larkin and G. Blatter, *Renormalization-group analysis of weak collective pinning in type-ii superconductors*, Phys. Rev. B **59** (1999) 11551–62.
[31] S. Stepanow, *Dynamics of growing interfaces in a disordered medium: the effect of lateral growth*, J. Phys. II (France) **5** (1995) 11–17.
[32] L. Balents and D.S. Fisher, *Large-N expansion of $4-\varepsilon$-dimensional oriented manifolds in random media*, Phys. Rev. **B 48** (1993) 5949–5963.
[33] P. Chauve, P. Le Doussal and K.J. Wiese, *Renormalization of pinned elastic systems: How does it work beyond one loop ?*, Phys. Rev. Lett. **86** (2001) 1785–1788.
[34] P. Le Doussal, K. Wiese and P. Chauve, *Two loop FRG study of pinned manifolds*, in preparation.
[35] P. Le Doussal and K. Wiese, *3-loop FRG study of pinned manifolds*, in preparation.
[36] P. Le Doussal and K.J. Wiese, *Functional renormalization group at large N for random manifolds*, cond-mat/**0109204** (2001).
[37] L.-H. Tang, M. Kardar and D. Dhar, *Driven depinning in anisotropic media*, Phys. Rev. Lett. **74** (1995) 920–3.
[38] R. Albert, A.-L. Barabasi, N. Carle and A. Dougherty, *Driven interfaces in disordered media: determination of universality classes from experimental data*, Phys. Rev. Lett. **81** (1998) 2926–9.
[39] P. Le Doussal and K. Wiese, *Functional renormalization group for anisotropic depinning and relation to some branching processes*, in preparation.
[40] D. Ertas and M. Kardar, *Critical dynamics of contact line depinning*, cond-mat/**9401027** (1994).
[41] M. Alava, *Scaling in self-organized criticality from interface depinning?*, J. Phys. Cond. Mat. **14** (2002) 2353.
[42] U. Schulz, J. Villain, E. Brezin and H. Orland, *Thermal fluctuations in some random field models*, J. Stat. Phys. **51** (1988) 1–27.
[43] T. Hwa and D.S. Fisher, *Anomalous fluctuations of directed polymers in random media*, Phys. Rev. B **49** (1994) 3136–54.
[44] A.A. Middleton and D.S. Fisher, *Critical behavior of pinned charge-density waves below the threshold for sliding*, Phys. Rev. Lett. **66** (1991) 92–5.
[45] A. Rosso and W. Krauth, *Origin of the roughness exponent in elastic strings at the depinning threshold*, Phys. Rev. Lett. **87** (2001) 187002.
[46] A. Rosso and W. Krauth, *Roughness at the depinning threshold for a long-range elastic string*, Phys. Rev. E **65** (2002) 025101/1–4.
[47] A. Rosso and W. Krauth, *Monte carlo dynamics of driven flux lines in disordered media*, cond-mat/**0107527** (2001).
[48] J.T. Chayes, L. Chayes, D.S. Fisher and T. Spencer, *Finite-size scaling and correlation lengths for disordered systems*, Phys. Rev. Lett. **57** (1986) 2999.
[49] S.N. Coppersmith and A.J. Millis, *Diverging strains in the phase-deformation model of sliding charge-density waves*, Phys. Rev. B **44** (1991) 7799–807.
[50] P. Le Doussal and T. Giamarchi, *Moving glass theory of driven lattices with disorder*, Phys. Rev. **B 57** (1998) 11356–11403.
[51] H. Leschhorn, *Interface depinning in a disordered medium-numerical results*, Physica A **195** (1993) 324–35.
[52] L. Roters, A. Hucht, S. Lubeck, U. Nowak and K.D. Usadel, *Depinning transition and thermal fluctuations in the random-field ising model*, Phys. Rev. E **60** (1999) 5202–7.
[53] U. Nowak and K.D. Usadel, *Influence of temperature on the depinning transition of driven interfaces*, Europhys. Lett. **44** (1998) 634–40.
[54] P. B. Thomas and M. Paczuski, *Avalanche dynamics of crack propagation and contact line depinning*, cond-mat/**9602023** (1996).
[55] L.-H. Tang and H. Leschhorn, *Pinning by directed percolation*, Phys. Rev. A **45** (1992) R8309–12.
[56] S.V. Buldyrev, A.-L. Barabasi, F. Caserta, S. Havlin, H.E. Stanley and T. Vicsek, *Anomalous interface roughening in porous media: experiment and model*, Phys. Rev. A **45** (1992) R8313–16.
[57] S.C. Glotzer, M.F. Gyure, F. Sciortino, A. Coniglio and H.E. Stanley, *Pinning in phase-separating systems*, Phys. Rev. E **49** (1994) 247–58.
[58] A. Hartmann A. Rosso and W. Krauth, in preparation.
[59] L. Roters and K.D. Usadel, submitted for publication.
[60] A. Prevost, E. Rolley and C. Guthmann, *Dynamics of a helium-4 meniscus on a strongly disordered cesium substrate*, Phys. Rev. B **65** (2002) 064517/1–8.
[61] D. Ertas and M. Kardar, *Anisotropic scaling in depinning of a flux line*, Phys. Rev. Lett. **73** (1994) 1703–6.
[62] S. Lemerle, J. Ferré, C. Chappert, V. Mathet, T. Giamarchi and P. Le Doussal, *Domain wall creep in an Ising ultrathin magnetic film*, Phys. Rev. Lett. **80** (1998) 849.
[63] P. Chauve and P. Le Doussal, *Exact renormalization group and applications to disordered problems: part i*, cond-mat/**9602023** (2000).
[64] L. Tang, unpublished.
[65] S. Ramanathan and D.S. Fisher, *Onset of propagation of planar cracks in heterogeneous media*, Phys. Rev. B **58** (1998) 6026–46.
[66] T. Giamarchi and P. Le Doussal, *Moving glass phases of driven lattices*, Phys. Rev. Lett. **76** (1996) 3408.
[67] A. Parisi, G. Caldarelli and L. Piotronero, *Roughness of fracture surfaces*, Europhys. Lett. **52** (2000) 304–10.
[68] M. Poujade, C. Guthmann and E. Rolley, submitted to Europhys. Lett. (2002). Preliminary report in J. of Low Temp. Phys. 126 (2002) 379.
[69] S. Moulinet, C. Guthmann and E. Rolley, in preparation; to be submitted to EPJ B.
[70] L. Bureau, T. Baumberger, C. Caroli, cond-mat/0101357.
[71] for a review see E. Bouchaud, J. Phys. Condensed Matter **9**, 4319 (1997), and Refs.[54,67].
[72] See e.g. S. Ramanathan and D.S. Fisher, condmat/9712181; S. Ramanathan, D. Ertas and D.S. Fisher, condmat/9611196, and references therein.
[73] A. Delaplace et al. Phys. Rev. E **60** 1337 (1999), P. Daguier et al. Europhys. Lett. 367 (1995).
[74] See e.g. E. Bouchaud et al., condmat/0108261, and references therein.
[75] We thank E. Brezin for a discussion on this point.
[76] If one excludes a rather unnatural scenario with $\int \Delta = O(\epsilon^2)$, where $\Delta(u) = \epsilon y_1(u) + \epsilon^2 y_2(u)$ with $y_1(u)$ corresponding to a 1-loop fixed point of range shorter than RF.
[77] L. Balents, P. Le Doussal in preparation.